

This document is the Accepted Manuscript version of a Published Work that appeared in final form in Inorganic Chemistry, copyright © American Chemical Society after peer review and technical editing by the publisher. To access the final edited and published work see <https://doi.org/10.1021/acs.inorgchem.1c02192>

# Lithiated calix[*n*]arenes (n = 6 or 8): Synthesis, structures, and use in the ring opening polymerization of cyclic esters

Tian Xing,<sup>a</sup> Chengying Jiang,<sup>b</sup> Mark R. J. Elsegood,<sup>b</sup> and Carl Redshaw<sup>a\*</sup>

<sup>a</sup> *Plastics Collaboratory, Department of Chemistry, University of Hull, Hull, HU6 7RX, U.K.*

<sup>b</sup> *Chemistry Department, Loughborough University, Loughborough, Leicestershire, LE11 3TU, U.K.*

**KEYWORDS:** calixarenes; lithiated complexes; ring opening polymerization of cyclic esters.

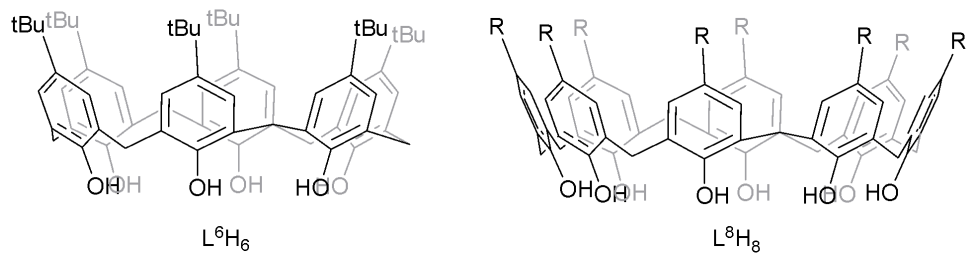
**ABSTRACT:** A variety of lithiated calix[*n*]arenes, for which n = 6 or 8, have been isolated, structurally characterized and evaluated as catalysts for the ring opening polymerization (ROP) of the cyclic esters  $\epsilon$ -caprolactone ( $\epsilon$ -CL),  $\delta$ -valerolactone ( $\delta$ -VL) and *r*-lactide (*r*-LA). In particular, interaction of *p*-*tert*-butylcalix[6]areneH<sub>6</sub> (L<sup>6</sup>H<sub>6</sub>) with LiOtBu in THF led to the isolation of [Li<sub>14</sub>(L<sup>6</sup>H)<sub>2</sub>(CO<sub>3</sub>)<sub>2</sub>(THF)<sub>6</sub>(OH<sub>2</sub>)<sub>6</sub>] $\cdot$ 14THF (**1**·14THF) the core of which has a chain of

5  $\text{Li}_2\text{O}_2$  diamonds. Similar use of *p-tert*-butylcalix[8]arene $\text{H}_8$  ( $\text{L}^8\text{H}_8$ ) afforded  $[\text{Li}_{10}(\text{L}^8)(\text{OH})_2(\text{THF})_8]\cdot 7\text{THF}$  (**2**·7THF), where the core is comprised of a six-rung Li – O ladder. Use of de-butylated calix[8]arene $\text{H}_8$  (deBu $\text{L}^8\text{H}_8$ ) led to an elongated dimer  $[\text{Li}_{18}(\text{deBuL}^8)_2(\text{OtBu})_2(\text{THF})_{14}]\cdot 4\text{THF}$  (**3**·4THF) in which the calix[8]arenes possess a wave-like conformation forming bridges to link three separate  $\text{Li}_x\text{O}_y$  clusters (where x and y = 6, ignoring the THF donor oxygens). Interaction of  $\text{L}^8\text{H}_8$  with  $\text{LiOH}\cdot\text{H}_2\text{O}$  afforded  $[\text{Li}_4(\text{L}^8\text{H}_4)(\text{OH})_4(\text{THF})_6]\cdot 5.5\text{THF}$  (**4**·5.5THF), where intramolecular H-bond interactions involving Li, O, and H construct a cage in the core of the structure with six and eight-membered rings. Lastly, addition of  $\text{Me}_3\text{Al}$  to the solution generated from  $\text{L}^8\text{H}_8$  and  $\text{LiOtBu}$  led to the isolation of  $[(\text{AlMe}_2)_2\text{Li}_{20}(\text{L}^8\text{H}_2)_2(\text{OH})_4(\text{O}^{2-})_4(\text{OH})_2(\text{NCMe})_{12}]\cdot 10\text{MeCN}$  (**5**·10MeCN) in which Li, O, Al, and N centers build a polyhedral core. These complexes have been screened for their potential to act as pre-catalysts in the ring opening polymerization (ROP) of  $\epsilon$ -CL,  $\delta$ -VL and *r*-LA. For the ROP of  $\epsilon$ -CL,  $\delta$ -VL, and *r*-LA, systems **1-4** exhibited moderate activity at 130 °C over 8 h. In the case of ROP using the mixed-metal (Li/Al) system **5**, better conversions and high molecular weight polymers were achieved. In the case of the ROP of  $\omega$ -pentadecalactone ( $\omega$ -PDL), the systems proved to be inactive under the conditions employed herein.

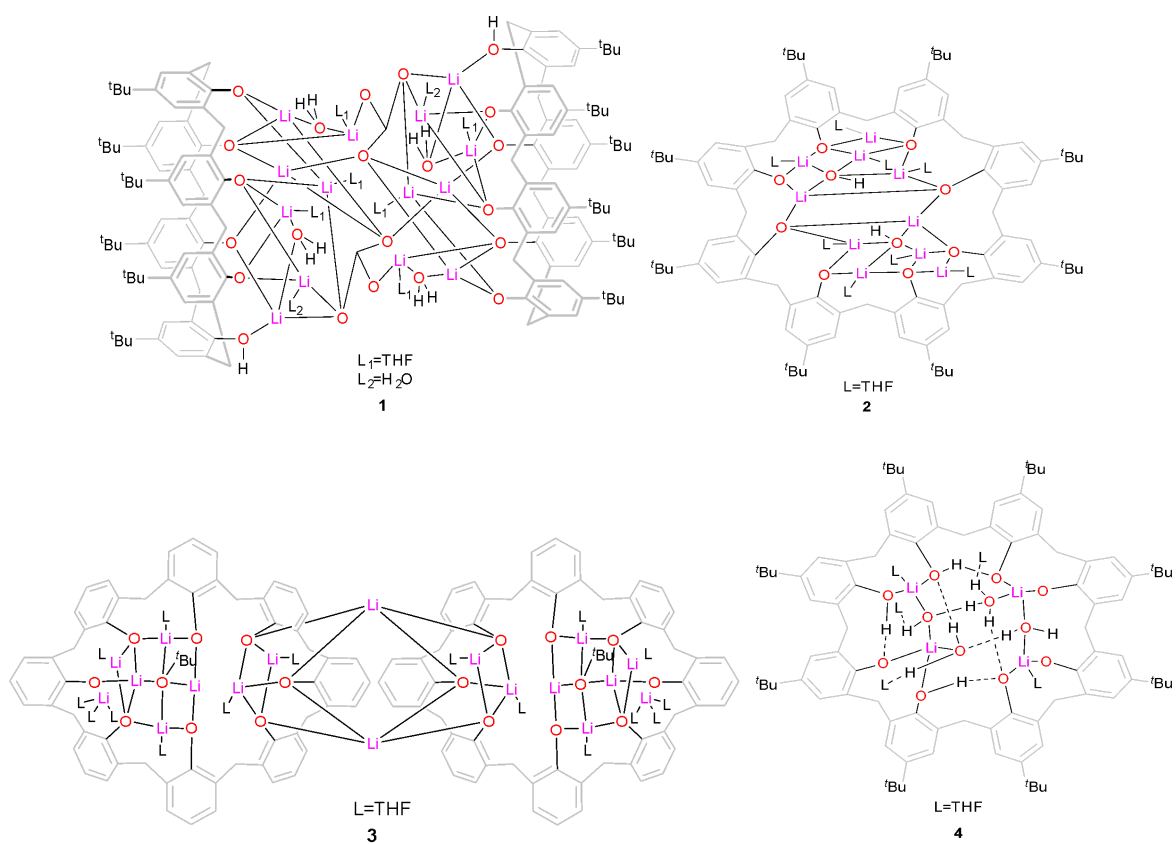
## 1. Introduction

The versatility of calixarenes is now well documented with applications ranging from their use in nuclear waste to use in hair dyes.<sup>[1-7]</sup> These uses stem from the facile functionalization of either the lower or upper rims, and the conformational flexibility displayed by such calixarenes which often results in the beneficial presence of  $\pi$ -rich cavities. Our interest stems from their ability to act as useful ancillary ligands in catalysis.<sup>[8]</sup> In recent work, we have reported that a family of

lithiated calix[4]arenes are capable of acting as efficient catalysts in the ring opening polymerization (ROP) of a number of cyclic esters, albeit with a lack of control.<sup>[9]</sup> This area is topical given the current issues with petroleum-based plastics, and the need to develop new polymeric materials with more environmentally friendly properties.<sup>[10]</sup> Studies have shown that larger calix[*n*]arenes have the ability to simultaneously bind multiple metal centers,<sup>[11]</sup> and, in the area of catalysis, this raises the possibility of the presence of beneficial cooperative effects. Mixed-metal systems can also exhibit interesting catalytic behavior, and it has been shown that the presence of one metal can impact on the catalytic potential of another.<sup>[12]</sup> In terms of the bigger calix[*n*]arenes, few lithiated species have appeared in the literature,<sup>[13,14]</sup> and none have been utilized in the ROP of cyclic esters. Reports include mixed lithium/strontium complexes available via the use of *n*BuLi with L<sup>8</sup>H<sub>8</sub> (or its *p-iso*-propyl analogue) and subsequent treatment with SrBr<sub>2</sub>.<sup>[13]</sup> Also, Fromm *et al* have structurally characterized the complex [Li<sub>2</sub>L<sup>8</sup>H<sub>6</sub>(THF)<sub>7</sub>(H<sub>2</sub>O)<sub>12</sub>]<sub>2</sub>, which resulted from the reaction of L<sup>8</sup>H<sub>8</sub> with Li<sub>2</sub>CO<sub>3</sub> in THF/water.<sup>[14]</sup> Herein, we have investigated reactions between *p-tert*-butylcalix[6 and 8]areneH<sub>6,8</sub> (L<sup>6</sup>H<sub>6</sub> and L<sup>8</sup>H<sub>8</sub>, Chart 1) and the lithium reagents Li*O**t*Bu or LiOH·H<sub>2</sub>O, and have isolated a number of intriguing multi-lithiated species, see chart 2. The bulk of our synthetic studies have focused on the L<sup>8</sup>H<sub>8</sub> system given its cost versus L<sup>6</sup>H<sub>6</sub> or *deBu*L<sup>8</sup>H<sub>8</sub>.<sup>[15]</sup> We note that lithiated species as catalysts for the ROP of cyclic esters has been reviewed,<sup>[16,17]</sup> whilst catalytic ROP systems based lithium-containing rings, cages and ladders have been reported.<sup>[18-27]</sup>



**Chart 1.** Calixarenes used in this study (R = H, *t*Bu).



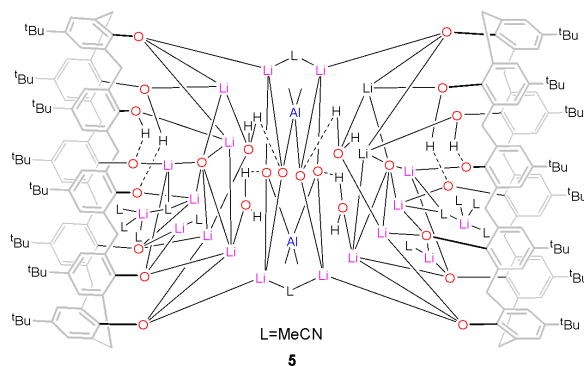


**Chart 2.** Pre-catalysts prepared herein.

## 2. Experimental section

### 2.1 Chemicals and apparatus

**Standard** Schlenk and cannula techniques including **the use of** a conventional nitrogen-filled glove-box **were employed throughout**. **The solvents used** were refluxed over an appropriate drying agent and **then** distilled/degassed prior to use. Elemental analyses were **conducted** by the **elemental analyses services team at** London Metropolitan University or **within** the Chemistry Department at the University of Hull. **A** Varian VXR 400 S spectrometer at 400 MHz or a Gemini at 300 MHz ( $^1\text{H}$ ) at 298 K **were employed to record the NMR spectra with** chemical shifts **referenced** to the residual protio impurity of the **solvent**. Perkin-Elmer 577 and 457 grating spectrophotometers **were used to record the IR spectra, which were run as nujol mulls between KBr plates**. All other **reagents** were **purchased from commercial sources** and **were** used as received unless stated otherwise.

**A** Bruker autoflex III smart beam in linear mode **was employed to obtain the** Laser Desorption/Ionization Time of Flight (MALDI-TOF) mass spectra, **which** were acquired by averaging at least 100 laser shots. **The matrix employed was** 2,5-dihydroxybenzoic acid **with**

THF as solvent, whilst the ionization agent used was sodium chloride in methanol. Sample preparation involved mixing 20  $\mu\text{L}$  of the matrix solution in THF (2  $\text{mg}\cdot\text{mL}^{-1}$ ) with 20  $\mu\text{L}$  of matrix solution (10  $\text{mg}\cdot\text{mL}^{-1}$ ) and 1  $\mu\text{L}$  of ionizing agent (1  $\text{mg}\cdot\text{mL}^{-1}$ ) solution. Following this, 1 mL of the respective mixture was deposited on a target plate and dried under air at ambient temperature.

### 2.2 Preparation of $[\text{Li}_{14}(\text{L}^6\text{H})_2(\text{CO}_3)_2(\text{THF})_6(\text{OH}_2)_6]\cdot 14\text{THF}$ (**1**·14THF)

A solution of lithium *tert*-butoxide (8.22 ml, 1.0M in THF, 8.22 mmol) was added to  $\text{L}^6\text{H}_6$  (1.00 g, 1.03 mmol) in THF (30 ml) at ambient temperature. After stirring for 4 h, concentration of the orange solution to 20 ml and standing for 48 h afforded small colorless crystals of the **1**·14THF in *ca* 15 % yield. Calcd for  $\text{C}_{158}\text{H}_{218}\text{Li}_{14}\text{O}_{30}$  (**1**·14THF–14THF requires C, 70.43; H, 8.15%); found C, 70.56; H, 7.89%. IR: 1616w, 1411w, 1365m, 1290w, 1261s, 1198w, 1095bs, 1020bs, 871w, 800bs, 736w, 721w, 704w, 661w.  $^1\text{H}$  NMR ( $\text{THF}_d$ , 400MHz)  $\delta$ : 7.24-6.79 (m, 12H, arylH), 4.35 (m, 4H,  $-\text{CH}_2-$ ), 3.72 (m, 4H,  $-\text{CH}_2-$ ), 3.36 (d, 2H,  $-\text{CH}_2-$ ), 3.24 (d, 2H,  $-\text{CH}_2-$ ), 2.66 (s, 12H,  $\text{H}_2\text{O}$ ), 1.69 (THF), 1.24-1.28 (m, 54H,  $\text{C}(\text{CH}_3)_3$ ).  $^7\text{Li}$  NMR ( $\text{THF}_d$ , 194.3 MHz, 298 K)  $\delta$ : 3.20 (bs), 2.72 (bs), 1.93 (s), 1.86 (s), 1.33 (s). Mass Spec (ED): 2177  $[\text{M}-6\text{H}_2\text{O}-20\text{THF}+\text{Na}^+]$ .

### 2.3 Preparation of $[\text{Li}_{10}(\text{L}^8)(\text{OH})_2(\text{THF})_8]\cdot 7\text{THF}$ (**2**·7THF)

A solution of lithium *tert*-butoxide (8.01 ml, 1.0M in THF, 8.01 mmol) was syringed into  $\text{L}^8\text{H}_8$  (1.00 g, 0.77 mmol) in THF (30 ml) at ambient temperature. Following stirring for 12h, the system was filtered and stored at 0 °C for 24h to afford **2**·7THF in *ca.* 50% yield. Calcd for

$C_{120}H_{170}Li_{10}O_{18}$  (**2**·7THF–7THF requires C, 73.16; H, 8.70%) found C, 72.69; H, 8.71%. IR: 3339bw, 3171bw, 2360w, 1738w, 1657m, 1614m, 1557m, 1297s, 1260s, 1202s, 1094bs, 1020bs, 872s, 804bs, 734s, 723s, 663m.  $^1H$  NMR (THF<sub>d8</sub>, 400MHz)  $\delta$ : 7.32-6.75 (m, 16H, arylH), 4.64 (overlapping d, 4H,  $-CH_2-$ ), 4.37 (d, 4H,  $-CH_2-$ ), 3.59 (THF), 3.20 (m, 4H,  $-CH_2-$ ), 3.04 (d, 4H,  $-CH_2-$ ), 1.74 (THF), 1.23 (s, 72H,  $C(CH_3)_3$ ).  $^7Li$  NMR (THF<sub>d8</sub>, 194.3 MHz, 298 K)  $\delta$ : 3.11 (s), 3.49 (bs), 3.61 (bs). Mass Spec (EI): 1416 [M–15THF+Na<sup>+</sup>].

#### 2.4 Preparation of $[Li_{18}(deBuL^8)_2(OtBu)_2(THF)_{14}] \cdot 4THF$ (**3**·4THF)

A solution of lithium *tert*-butoxide (12.25 ml, 1.0M in THF, 12.2 mmol) was syringed into  $deBuL^8H_8$  (1.00 g, 1.18 mmol) in THF (30 ml) at ambient temperature. Following stirring for 4 h, filtration and prolonged standing (1 week) at ambient temperature afforded colorless prisms of **3**·4THF (in *ca.* 35% yield). Anal. Calcd for  $C_{184}H_{226}Li_{18}O_{34}$  (sample dried *in-vacuo* for 12 h, –4THF) requires C, 71.14; H, 7.33%. Found C 70.96, H 7.22%. IR: 2727w, 1589m, 1460s, 1436s, 1377s, 1261s, 1091s, 1041s, 1019s, 907w, 840m, 799s, 752m, 722w, 695w.  $^1H$  NMR (THF<sub>d8</sub>, 400MHz)  $\delta$ : 7.14-6.89 (m, 16H, arylH), 4.54 (d, 4H,  $-CH_2-$ ), 4.44 (d, 4H,  $-CH_2-$ ), 4.29 (d, 4H,  $-CH_2-$ ), 4.14 (d, 4H,  $-CH_2-$ ) 3.56 (THF), 3.22-3.32 (m, 8H,  $-CH_2-$ ), 1.74 (THF), 1.12 (s, 18H,  $-OC(CH_3)_3$ ).  $^7Li$  NMR (THF<sub>d8</sub>, 194.3 MHz, 298 K)  $\delta$ : 4.87 (s), 4.10 (s), 1.27 (bs). Mass spec (EI): 1066 [(M–18THF)/2 –Li<sup>+</sup>+Na<sup>+</sup>].

#### 2.5 Preparation of $[Li_4(L^8H_4)(OH)_4(THF)_6] \cdot 5.5THF$ (**4**·5.5THF)

THF (30 mL) was transferred into a Schlenk containing  $L^8H_8$  (1.00 g, 0.77 mmol) and LiOH·H<sub>2</sub>O (0.07 g, 1.67 mmol), and refluxed for 12h. On cooling, the system was filtered and allowed to stand at 0 °C to afford **4**·5.5THF in *ca.* 28% yield. Calcd for  $C_{112}H_{156}Li_4O_{14}$

(4.5THF–5.5THF–4H<sub>2</sub>O requires C, 76.69; H, 8.96%), found C, 76.89; H, 9.05%. IR: 2727w, 2359m, 1620w, 1614w, 1539w, 1462s, 1414w, 1377s, 1260s, 1093s, 1019s, 872w, 799s, 739w, 722w. <sup>1</sup>H NMR (THF<sub>d8</sub>, 400 MHz) δ: 7.11-6.92 (m, 16H, arylH), 4.72 (d, 4H, -CH<sub>2</sub>-), 4.40 (d, 8H, -CH<sub>2</sub>-), 3.57 (THF), 3.35 (s, 4H, OH), 3.20 (d, 4H, -CH<sub>2</sub>-), 2.60 (s, 4H, H<sub>2</sub>O), 1.73 (THF), 1.22-1.28 (overlapping s, 72H, C(CH<sub>3</sub>)<sub>3</sub>). <sup>7</sup>Li NMR (THF<sub>d8</sub>, 194.3 MHz, 298 K) δ: 3.55 (s). Mass Spec. (EI): 1645 [M–2H<sub>2</sub>O–7.5THF].

#### 2.6 Preparation of [(AlMe<sub>2</sub>)<sub>2</sub>Li<sub>20</sub>(L<sup>8</sup>H<sub>2</sub>)<sub>2</sub>(OH<sub>2</sub>)<sub>4</sub>(O<sup>2-</sup>)<sub>4</sub>(OH)<sub>2</sub>(NCMe)<sub>12</sub>] $\cdot$ 10MeCN (**5** $\cdot$ 10MeCN)

Lithium *tert*-butoxide (8.01 ml, 1.0M in THF, 8.01 mmol) was syringed into L<sup>8</sup>H<sub>8</sub> (1.00 g, 0.77 mmol) in THF (30 ml) at ambient temperature. After stirring for 1 h, Me<sub>3</sub>Al (1.0M, 1.50 mmol) was added to the orange solution, which was then refluxed for a further 12 h. Following this, the volatiles were evaporated *in-vacuo*, and the remaining residue was extracted into MeCN (30 ml). Standing at ambient temperature for 48h led to the formation of colorless crystals of **5** $\cdot$ 10MeCN in *ca* 20 % yield. Calcd for C<sub>196</sub>H<sub>258</sub>Al<sub>2</sub>Li<sub>20</sub>O<sub>26</sub>N<sub>8</sub> (**5** $\cdot$ 10MeCN–14MeCN requires C, 70.59; H, 7.80; N, 3.35%), found C, 70.74; H, 7.45; N 3.03%. IR (MeCN product): 2727w, 2261w, 1700w, 1657w, 1604w, 1462s, 1377m, 1362m, 1296m, 1260s, 1296m, 1260s, 1207m, 1093s, 1019s, 909w, 872w, 800s. <sup>1</sup>H NMR (THF<sub>d8</sub>, 400MHz) δ: 7.19-6.93 (m, 32H, arylH), 4.54 (d, 8H, -CH<sub>2</sub>-), 4.38 (d, 8H, -CH<sub>2</sub>-), 4.27 (d, 8H, -CH<sub>2</sub>-), 4.14 (d, 4H, -CH<sub>2</sub>-), 3.25 (s, 2H, OH), 3.20 (m, 4H, -CH<sub>2</sub>-), 2.47 (s, 8H, H<sub>2</sub>O), 1.91 (s, 12H, MeCN), 1.28-1.13 (overlapping s, 144H, C(CH<sub>3</sub>)<sub>3</sub>), -0.81 (s, 12H, AlMe<sub>2</sub>); calixOH not observed. <sup>7</sup>Li NMR (THF<sub>d8</sub>, 194.3 MHz, 298 K) δ: 5.18 (bs), 4.75 (bs), 4.43 (s), 3.88(s). Mass spec. (EI): 1527 [(M-22MeCN)/2+Na<sup>+</sup>].

#### 2.7 Procedure for the ROP of $\epsilon$ -caprolactone, $\delta$ -valerolactone and *rac*-lactide

A solution of the respective pre-catalyst (0.010 mmol, 1.0 mL toluene) was syringed into a Schlenk flask in the glove-box at ambient temperature. After stirring for 2 min, the appropriate amount of BnOH (using a pre-prepared 100 mL stock toluene solution containing 1 mmol BnOH) and of  $\epsilon$ -CL,  $\delta$ -VL, or *r*-LA together with 1.5 mL toluene was added. The Schlenk flask was then heated at 130 °C using an oil/sand bath, and stirred for the required time, namely 8 or 24 h. Following this, the mixture was quenched by addition of an excess of glacial acetic acid (0.2 mL), and then the resultant solution was then poured into a beaker of cold methanol (200 mL, 0 °C). The polymer product was collected on filter paper and dried *in-vacuo*.

*Solvent-free conditions:* Under an inert atmosphere, a THF solution of the complex (1 mM) was added into a Schlenk tube and the solvent was removed using the vacuum line at ambient temperature. The monomer (9.0 mmol) was then added, and the reaction was stirred at 130 °C for 12-24 h, or until a mass of polymer blocking the stirring formed. The mixture was then taken up in CH<sub>2</sub>Cl<sub>2</sub> and quenched with acidified methanol (200 mL). The polymer product was isolated on a filter paper and then dried under air at ambient temperature.

## 2.8 Kinetic studies

For the polymerizations, the conditions were set up as 130 °C in toluene (2 mL) using 0.010 mmol of complex, using a molar ratio of monomer to initiator to co-catalyst of 500:1:1. At appropriate regular time intervals, and under a blanket of N<sub>2</sub>, 0.5  $\mu$ L aliquots were taken out and these were quenched using wet CDCl<sub>3</sub>. The degree of conversion of monomer to polymer was calculated via <sup>1</sup>H NMR spectroscopy.

## 2.9 Crystal Structure Determinations

Diffraction data were measured on sealed tube sources for **1**·14THF & **2**·7THF, rotating anode sources for **3**·4THF & **5**·10MeCN, and using synchrotron radiation for **4**·5.5THF. Data were corrected for absorption and structures solved by a charge-flipping algorithm. **The** non-H atoms were refined anisotropically and a riding model was used for all H atoms except those on heteroatoms when the quality of the data permitted. <sup>[28]</sup> In general, these lithium calixarenes crystals are very weakly diffracting due to the lack of any heavy elements and their inherently large unit cells. They are also subject the usual difficulties encountered with calixarene crystallography, namely *t*Bu group and solvent of crystallisation disorder, as well as a significant solvent of crystallisation loading. **In each case, the amount** of solvent molecules of crystallization should therefore be regarded as approximate. Where disorder was **accounted for**, restraints were applied to anisotropic displacement parameters and geometry. In pathological cases, Platon Squeeze was used to **account for** badly disordered solvent molecules as diffuse regions of electron density and this solvent was accounted for in the formula. <sup>[29,30]</sup>

For **1**·14THF, *t*Bu groups at C(18), C(29), C(51), and C(62), were modelled with the methyl groups split over two sets of positions with major occupancies of 84.8(16), 52(3), 73.9(14), and 74(3)%, respectively. In the THF containing O(22), atoms C(105) & C(106) were accounted for as split over two sets of positions with major occupancy 59(2)%. Geometric and vibration parameter restraints were applied to some badly behaved THF molecules. Distance restraints were applied to assist geometry in two of the water molecules. There remains some unresolved

disorder, and hence some less than ideal geometry, in some of the non-coordinated THF molecules.

For **2·7THF**, in each calix[8]arene complex molecule there are eight bonded molecules of THF and seven THF solvent of crystallization of which four are well defined (two of these unique). Twelve molecules of THF were accounted for per unit cell as a diffuse area of electron density by the Platon Squeeze procedure, *i.e.* three extra per calixarene complex.<sup>[29,30]</sup> Four THFs lie above the calixarene plane, two are in calixarene cavities and two lie in clefts within the calixarene's undulating ruffles. Three unique *t*Bu groups modelled as disordered over two sets of positions: including that at C(7), with major component = 78.7(6)%; that including C(18) with major component = 66.6(7)%; that including C(40) with major component = 80(4)%. Five THFs were disordered: that including O(6): C(46) split with major component = 50.9(17)%; that including O(8): C(54) split with major component = 51.3(19)%; that including O(9): all C atoms split with major component = 58.4(9)%; that including O(10): all C & O atoms split except C(62) with major component = 71.0(7)%; that including O(11): O(11) & C(68) split with major component = 50.7(14)%.

For **3·4THF**, in each calix[8]arene complex molecule there are 16 Li-coordinated THF molecules and 2 *Ot*Bu groups. 8 molecules of THF were accounted for per unit cell as a diffuse area of electron density by the Platon Squeeze procedure.

For **4·5.5THF**, in each *t*Bucalix[8]arene complex molecule there are two Li-bonded molecules of THF. 8 THF solvent molecules of crystallization were accounted for as point atoms per complex molecule, of which 4 are H-bonded to the calixarene complex molecule. One and a half

molecules of THF were modelled as diffuse areas of electron density by the Platon Squeeze procedure. Two THFs including O(10) {C(58) & C(59) split} and O(11) {C(62) – C(64) split} were accounted for as disordered over two sets of positions with major components = 81.6(13)% and 60.3(17)% respectively.

For **5**·10MeCN, the *t*Bu group including C(15) > C(18) was modelled as disordered over two sets of positions: with major component = 67.3(12)%; part of a calixarene ring and *t*Bu group including C(33) > C(35) & C(37) > C(40) was also modelled as 2-fold disordered with major component = 73.5(11)%, *t*Bu group C(47) > C(49) was disordered across a symmetry element, so was modelled at 50% occupancy; the MeCN including N(1) was also modelled as disordered with major component = 56.7(10)% while that including N(8) was similarly disordered in the vicinity of MeCN including N(1), so their occupation factors were linked.

### 3. Result and discussion

#### 3.1. Syntheses and solid-state structures

Using a modification of the method reported by Fromm *et al.* for the complex [Li<sub>4</sub>(*p*-*tert*-butylcalix[4]arene)(THF)<sub>4</sub>]<sub>2</sub>·6THF,<sup>[31]</sup> we treated L<sup>6</sup>H<sub>6</sub> with LiO*t*Bu in THF at ambient temperature. Following stirring (4h) and concentration of the solution, the complex [Li<sub>14</sub>(L<sup>6</sup>H)<sub>2</sub>(CO<sub>3</sub>)<sub>2</sub>(THF)<sub>6</sub>(OH<sub>2</sub>)<sub>6</sub>]<sub>2</sub>·14THF (**1**·14THF) was isolated as the only crystalline product in low yield (*ca.* 15%). The molecular structure is illustrated in Figure 1, and selected bond lengths and angles are provided in the caption. The molecule lies on a centre of symmetry, and thus half of the formula above is the asymmetric unit. <sup>1</sup>H NMR spectroscopic data are consistent with the solid-state structure, whilst in the <sup>7</sup>Li NMR spectrum, only 5 distinct lithium resonances

are observed. In the EI mass spectrum, a peak is observed at 2177 Da assigned to the molecular ion  $-6\text{H}_2\text{O}-20\text{THF}+\text{Na}^+$ .

The presence of the bridging  $\text{CO}_3^{2-}$  anions in the structure is not unprecedented, and has been reported elsewhere in metal phenolate chemistry. For example, McIntosh, Brechin, and Dalgarno *et al.* utilized bis-phenolate 6,6'-methylenebis(4-*tert*-butyl)-2-(hydroxymethyl)phenol to form a cobalt ( $\text{Co}_{15}$ ) cluster, the structure of which was found to incorporate a  $\mu_6\text{-CO}_3^{2-}$  ligand. The carbonate in this  $\text{Co}_{15}$  cluster was thought to arise via the incorporation of atmospheric  $\text{CO}_2$ , which, given the limited solubility of the  $\text{CO}_2$  under the conditions employed, led to a low product yield.<sup>[32]</sup> In **1**·14THF, we observe a similarly low yield, and also propose that the carbonate incorporation stems from exposure to atmospheric  $\text{CO}_2$ . In **1**·14THF, one calixarene oxygen, namely O(2), retains a proton and forms an H-bond with a neighboring phenolate oxygen, O(1). The H atoms of water molecule at O(9) form H-bonds with a calixarene phenolate oxygen O(3A) and a THF oxygen. Water molecules at O(8) & O(9) bridge pairs of  $\text{Li}^+$  ions, while that at O(7) is terminal. The H atoms of the water molecule at O(8) form an H-bond with a calixarene phenolate oxygen O(5) and an  $\text{O-H}\cdots\pi$  interaction with the aromatic ring C(34) > C(39) of the calixarene at a distance of 2.37 Å. The water molecule at O(7) forms an H-bond with a THF oxygen for one H atom, but no non-covalent interaction with the other H. There are some clear methylene H atom interactions with  $\text{Li}^+$  centers, for example at Li(7) with H(55B) = 2.12 Å, Li(1) with H(66A) = 2.25 Å, and Li(4) with H(33B) = 2.17 Å. The carbonate ions form bonds to a total of 7  $\text{Li}^+$  ions each. Each  $\text{Li}^+$  is essentially 4-coordinate, ignoring the interactions with H atoms. Li(2), Li(5), and Li(7) each bind to a terminal THF ligand. The core of the molecule is an elongated array of 14 oxygen-bridged  $\text{Li}^+$  ions approx. 12 Å long. The core of the

molecule has a chain of 5  $\text{Li}_2\text{O}_2$  diamonds (see figure 2). In terms of charge, the 14+ available from the Li centers is balanced by 10- from the two calix[6]arenes and 4- from the two  $\text{CO}_3^{2-}$  anions.

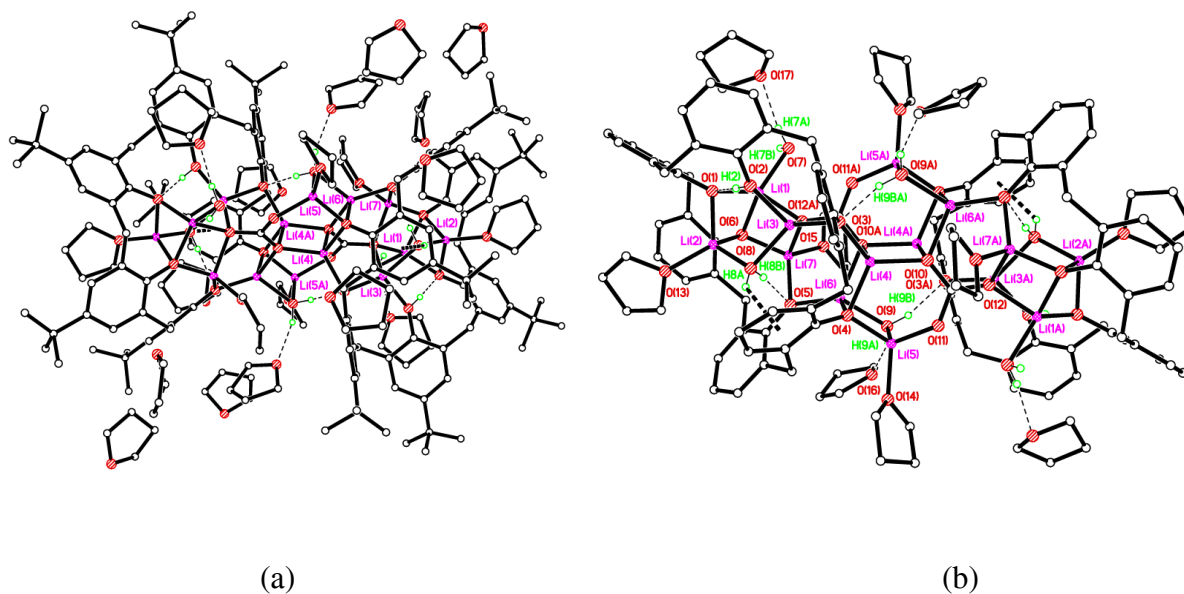


**Figure 1.** Two views showing the molecular structure of  $[\text{Li}_{14}(\text{L}^6\text{H})_2(\text{CO}_3)_2(\text{THF})_6(\text{OH}_2)_6]\cdot 14\text{THF}$  (**1**·14THF). View (b) also has calixarene *t*Bu groups and unbound THFs omitted. The majority of H atoms and minor disorder components are omitted for clarity. Views (a) and (b) Selected bond lengths (Å) and angles (°): Li(1)–O(6) 1.933 (12), Li(1)–O(7) 1.954(14), Li(1)–O(1) 1.954 (13), Li(2)–O(1) 1.905(13), Li(2)–O(13) 1.939 (13), Li(3)–O(3) 1.932 (11), Li(3)–O(8) 2.103 (12), Li(4)–O(3) 1.931(12), Li(4)–O(10) 1.959(11), Li(5)–O(4) 1.874(12), Li(5)–O(11) 1.876(11), Li(6)–O(5) 1.924(11), Li(6)–O(4) 1.995(13), Li(7)–O(6) 1.850(11), Li7–O5 1.901(13), O(6)–Li(1)–O(1) 92.0(5), O(7)–Li(1)–O(1) 124.1(7), O(1)–Li(2)–O(13) 114.8(6) O(1)–Li(2)–O(6) 91.7(6), O(3)–Li(3)–O(2) 113.2(6), O(3)–Li(4)–O(10) 124.5(6), O(3)–Li(4)–O(4) 116.5(5). Symmetry code A =  $-x+1, -y+1, -z+2$ .

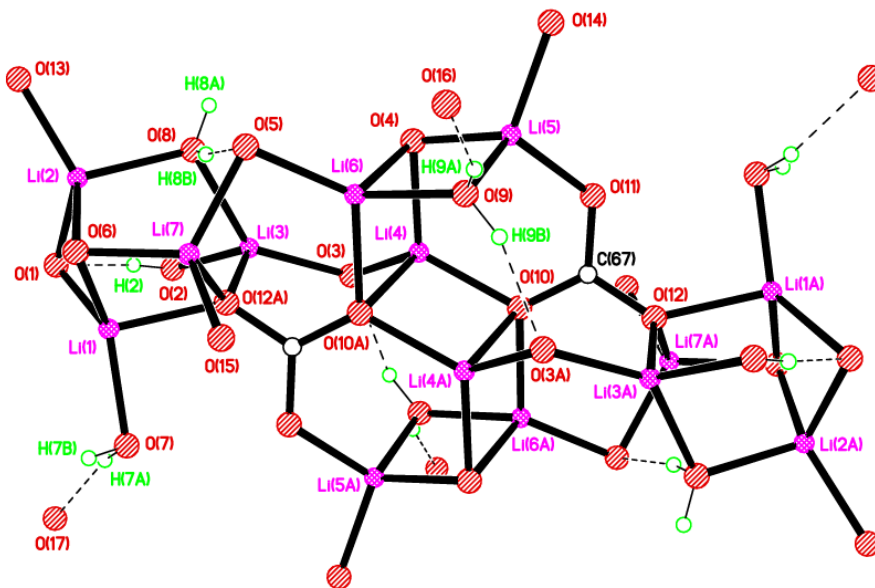


**Figure 2.** The core of  $[\text{Li}_{14}(\text{L}^6\text{H})_2(\text{CO}_3)_2(\text{THF})_6(\text{OH}_2)_6] \cdot 14\text{THF}$  (**1**·14THF).

The treatment of  $\text{L}^8\text{H}_8$  with  $\text{LiO}t\text{Bu}$  in THF at ambient temperature afforded  $[\text{Li}_{10}(\text{L}^8)(\text{OH})_2(\text{THF})_8] \cdot 7\text{THF}$  (**2**·7THF) in moderate isolated yield (*ca.* 50%). The molecular structure is presented in Figure 3, and selected bond lengths and angles are provided in the caption. It is a twinned data set with two twin components related by  $177.5^\circ$  rotation about reciprocal axis  $[0\ 1\ 0]$ . The molecule resides on a center of symmetry, and thus half is unique. The core consists of a six-rung Li – O ladder, and Li(1), Li(2), Li(3), Li(4), and Li(5) all have four bonds which connect with oxygen (for alternative views of the core see figure S1, ESI). There is H-bonding involving two of the Li-bound (at Li(4)/Li(4A)) THFs. Each molecule has two intramolecular H-bonded interactions between oxygen (in THF) to the hydroxyl H. In the  $^7\text{Li}$  NMR spectrum, we observed only 3 distinct lithium resonances, whilst in the EI mass spectrum, a peak is observed at 1416 Da is assigned to the molecular ion  $-15\text{THF} + \text{Na}^+$ . In terms of charge,

the 10+ available from the Li centers is balanced by 8- from the calix[8]arene and 2- from the two OH<sup>-</sup> anions.

Similar use of de-butylated calix[8]areneH<sub>8</sub> (deBuL<sup>8</sup>H<sub>8</sub>) led to an elongated dimer [Li<sub>18</sub>(deBuL<sup>8</sup>)<sub>2</sub>(OtBu)<sub>2</sub>(THF)<sub>14</sub>].4THF (**3·4THF**). The molecular structure is displayed in Figure 4, and selected bond lengths and angles are provided in the caption. The molecule resides on a center of symmetry. Two calix[8]arene ligands, which possess a wave-like conformation, form bridges to link three separate Li<sub>x</sub>O<sub>y</sub> clusters. Li(1), Li(2), Li(4), Li(6), Li(8), and Li(9) all have four bonds which connect with oxygen, whilst Li(3), Li(5), and Li(7) have three bonds; a view of the core is given in Figure 5. Li(7) makes some weak π interactions with C atoms in the neighboring calixarene rings attached to O(1) and O(7). In terms of charge, the 18+ available from the Li centers is balanced by 16- from the two calix[8]arenes and 2- from the two OtBu<sup>-</sup> anions.

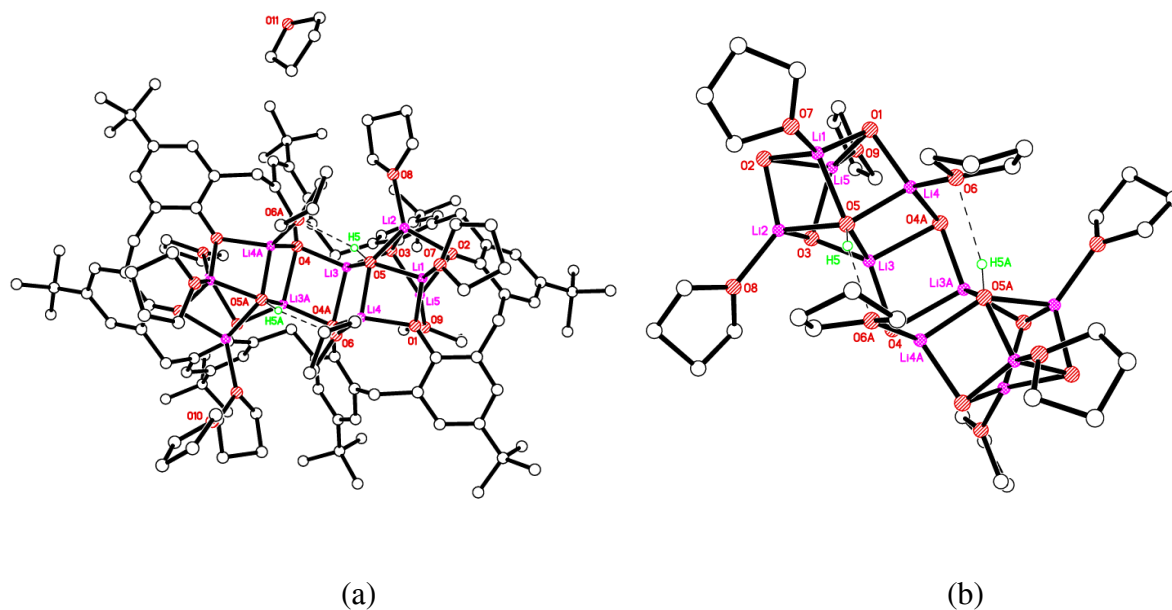


**Figure 3.** Molecular structure (a) and core (b) of [Li<sub>10</sub>(L<sup>8</sup>)(OH)<sub>2</sub>(THF)<sub>8</sub>].7THF (**2·7THF**). The majority of H atoms and minor disorder components are omitted for clarity. Selected bond

lengths (Å) and angles (°): Li(1)–O(1) 1.896(5), Li(1)–O(2) 1.896(5), Li(1)–O(5) 1.956(5), Li(2)–O(2) 1.911(5), Li(2)–O(3) 1.874(5), Li(2)–O(8) 1.939(5), Li(3)–O(3) 1.920(5), Li(3)–O(4) 1.940(5), Li(3)–O(5) 1.991(5); O(1)–Li(1)–O(2) 97.9(2), Li(1)–O(5)–Li(3) 130.3(2), Li(3)–O(4)–Li(4A) 110.0(2). Symmetry code A =  $-x+0.5, y, -z+1$ .

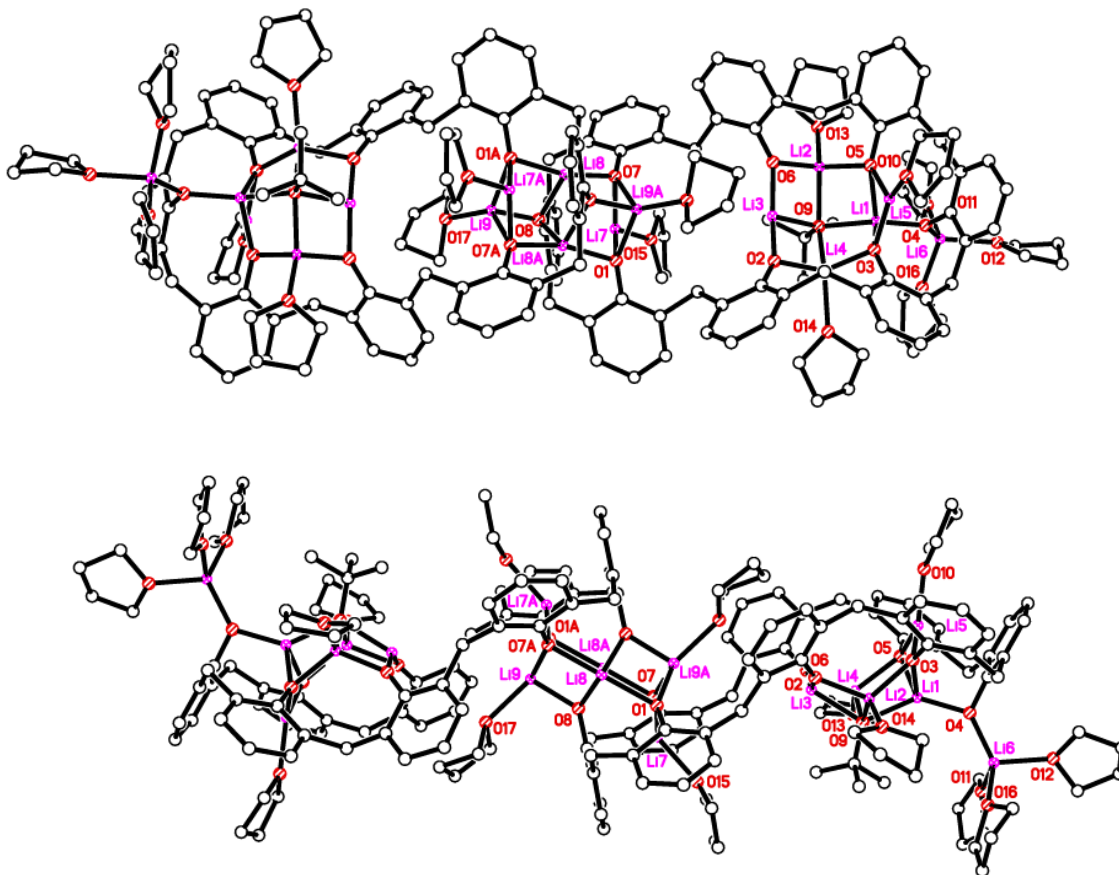


**Figure 4.** Two views, rotated by approx. 90°, of the molecular structure of  $[\text{Li}_{18}(\text{deBuL}^8)_2(\text{OtBu})_2(\text{THF})_{14}] \cdot 4\text{THF}$  (**3**·4THF). H atoms and non-coordinated THFs omitted for clarity. Selected bond lengths (Å) and angles (°): Li(1)–O(3) 1.977(15), Li(1)–O(4) 1.838(16), Li(1)–O(5) 2.056(13), Li(1)–O(9) 2.029(18), Li(2)–O(5) 2.056(13), Li(2)–O(6) 1.815(15), Li(2)–O(9) 2.061(14), Li(2)–O(13) 2.031(14), Li(3)–O(2) 1.778(12), Li(3)–O(6) 1.833(12), Li(3)–O(9) 2.056(14), Li(4)–O(2) 1.900(15), Li(4)–O(3) 1.972(17), Li(4)–O(9) 2.054(13), Li(5)–O(3) 1.839(16), Li(5)–O(5) 1.923(14), Li(6)–O(4) 1.885(16), Li(7)–O(1) 1.901(13), Li(7)–O(7) 1.937(13), Li(8)–O(7) 2.043(15), Li(8)–O(8) 1.951(15); Li(1)–O(3)–Li(4) 82.0(7),

Li(1)–O(3)–Li(5) 78.5(6), Li(1)–O(4)–Li(6) 133.6(8), Li(1)–O(9)–Li(3) 123.9(6). Symmetry code A =  $-x+1, -y+1, -z+1$ .

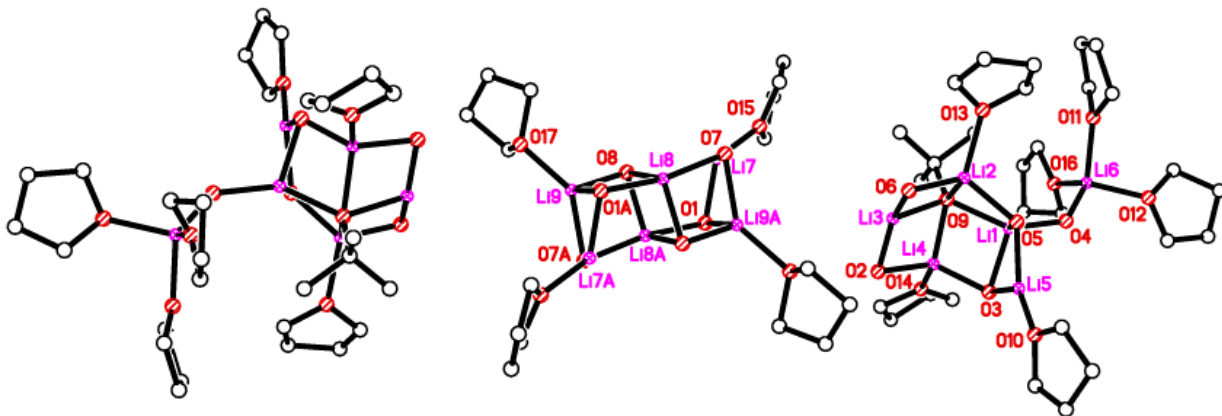


**Figure 5.** Three views showing the core of  $[\text{Li}_{18}(\text{deBuL}^8)(\text{OtBu})_2(\text{THF})_{14}] \cdot 4\text{THF}$  ( $3 \cdot 4\text{THF}$ ). Unbound solvent molecules and hydrogen atoms have been omitted for clarity.

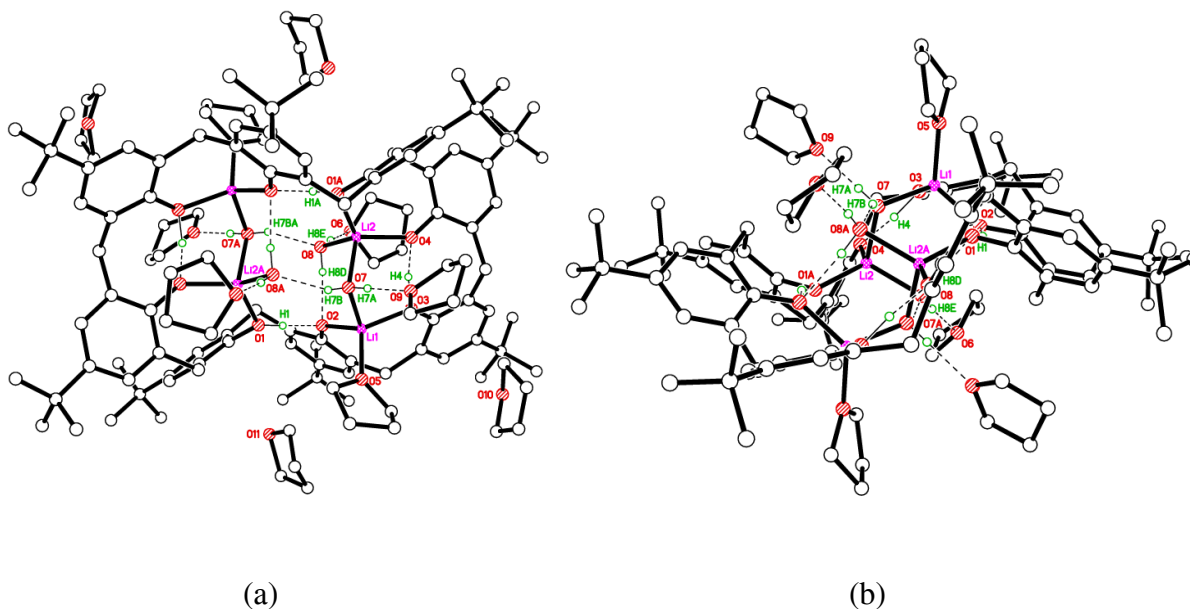


**Figure 6.** Two approx. perpendicular views showing the molecular structure of  $[\text{Li}_4(\text{L}^8\text{H}_4)(\text{OH}_2)_4(\text{THF})_6] \cdot 5.5\text{THF}$  ( $4 \cdot 5.5\text{THF}$ ). The majority of H atoms and minor disorder

components have been omitted for clarity. Selected bond lengths (Å) and angles (°): Li(1)–O(2) 1.900(7), Li(1)–O(3) 1.931(8), Li(1)–O(7) 1.970(8), Li(2)–O(1A) 1.922(8), Li(2)–O(4) 1.905(7), Li(2)–O(8) 1.971(8); Li(1)–O(7)–Li(2) 103.6(3), O(1A)–Li(2)–O(8) 112.5(3), O(4)–Li(2)–O(8) 114.8(4). Symmetry code A =  $-x+1, -y+1, -z+1$ .

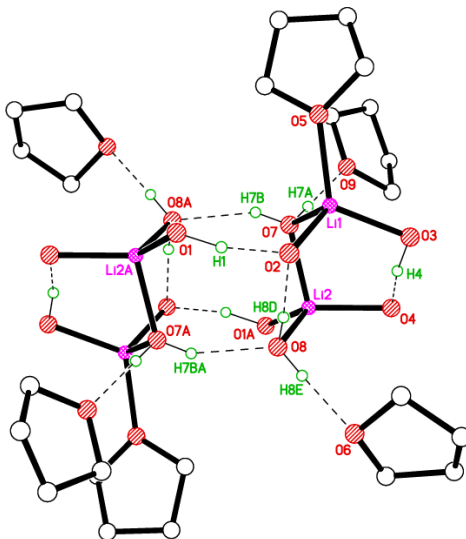


**Figure 7.** A view showing the core in  $[\text{Li}_4(\text{L}^8\text{H}_4)(\text{OH}_2)_4(\text{THF})_6] \cdot 5.5\text{THF}$  (**4·5.5THF**).

Interaction of  $\text{L}^8\text{H}_8$  with  $\text{LiOH} \cdot \text{H}_2\text{O}$  afforded  $[\text{Li}_4(\text{L}^8\text{H}_4)(\text{OH}_2)_4(\text{THF})_6] \cdot 5.5\text{THF}$  (**4·5.5THF**). Crystals of suitable quality for an X-ray diffraction study were afforded from a saturated THF solution on standing at room temperature. The molecular structure is presented in Figure 4, and selected bond lengths and angles are provided in the caption. The molecule resides on a center of symmetry, thus half is unique. The calix[8]arene adopts a wave-like conformation. Both the Li(1) and Li(2) centers have four bonds which connect with oxygen. A view of the core is given in figure 7; an alternative view is provided in the ESI (see figure S2). Hydrogens on water O(7)

H-bond to oxygen on the THF, including O(9) and water molecule O(8A). Hydrogens on water O(8) H-bond to oxygen on calixarene O(2) (phenolate, which has strong electronegativity) and oxygen on the THF, including O(6). The intramolecular H-bond interactions involving Li, O, and H construct a cage in the core of the structure with six and eight-membered rings. In the  $^7\text{Li}$  NMR spectrum, only one peak was observable, whilst in the EI mass spectrum, a peak observed at 1645 Da is assigned to the molecular ion  $-2\text{H}_2\text{O}-7.5\text{THF}$ . In terms of charge, the 4+ available from the Li centers is balanced by 4- from calix[8]areneH<sub>4</sub>.

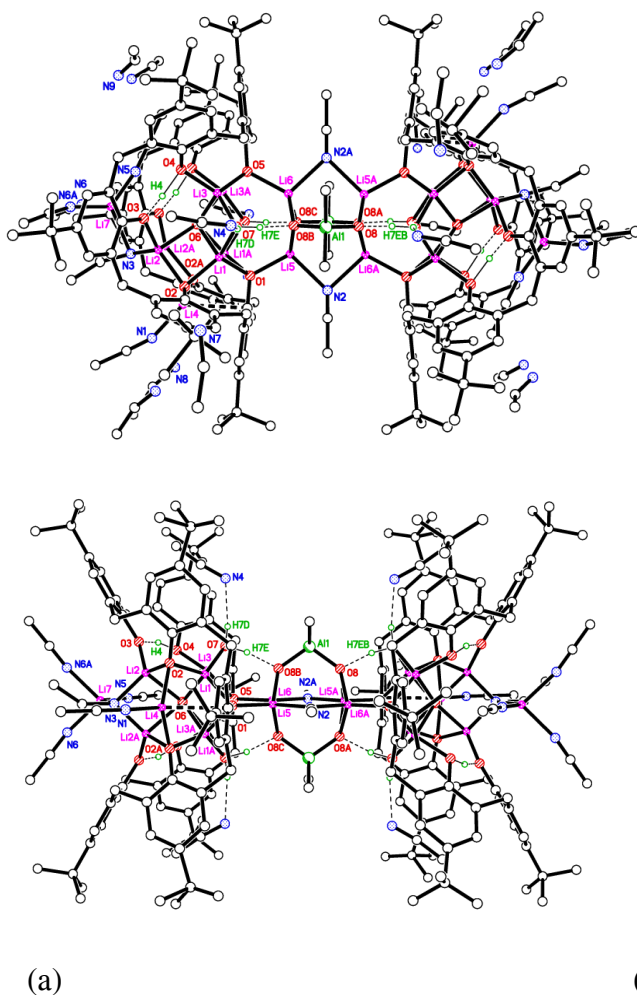


**Figure 8.** Two perpendicular views showing the molecular structure of  $[(\text{AlMe}_2)_2\text{Li}_{20}(\text{L}^8\text{H}_2)_2(\text{OH}_2)_4(\text{O}^{2-})_4(\text{OH})_2(\text{NCMe})_{12}] \cdot 10\text{MeCN}$  (**5**·10MeCN). The majority of H atoms and minor disorder components are omitted for clarity. Selected bond lengths (Å) and

angles (°): Li(1)–O(1) 1.917(7), Li(1)–O(2) 1.885(7), Li(1)–O(6) 2.074(7), Li(1)–O(7) 1.901(7), Li(2)–O(2) 1.902(8), Li(2)–O(3) 1.878(8), Li(2)–O(6) 2.195(8), Li(2)–N(3) 1.864(9), Li(3)–O(4) 1.904(7), Li(3)–O(5) 1.929(7), Li(3)–O(6) 2.089(7), Li(3)–O(7) 1.925(7), Li(4)–O(2) 1.993(8), Li(4)–N(1) 1.920(18), Li(5)–O(1) 1.906(9), Li(5)–N(2) 2.173(9), Li(6)–O(5) 1.939(9), Al(1)–O(8) 1.626(2); O(8)–Al(1)–O(8B) 108.82(18), Li(1)–O(1)–Li(5) 109.1(3), Li(1)–O(1)–Li(1A) 81.5(4), Li(2)–O(2)–Li(4) 93.5(6). Symmetry operators to generate the whole molecule from the quarter that is unique: (i)  $-x, -y, z$ ; (ii)  $x, y, -z$ ; (iii)  $-x, -y, -z$ .

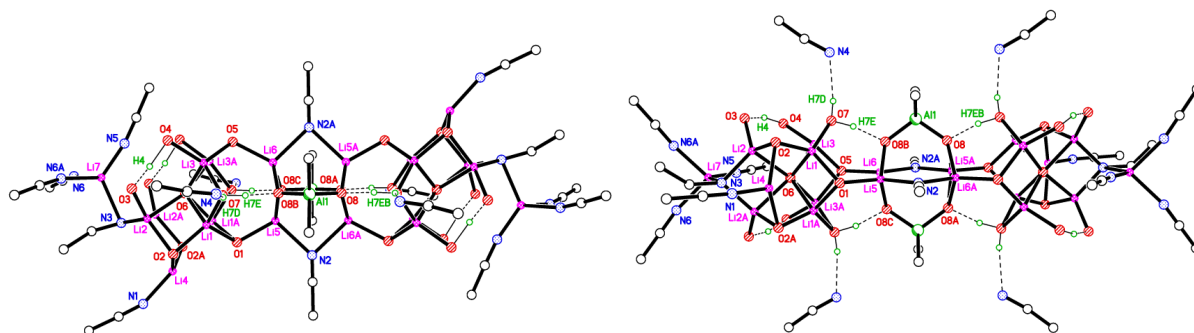


**Figure 9.** Two representations showing the core in  $[(\text{AlMe}_2)_2\text{Li}_{20}(\text{L}^8\text{H}_2)_2(\text{OH}_2)_4(\text{O}^{2-})_4(\text{OH})_2(\text{NCMe})_{12}] \cdot 10\text{MeCN}$  (**5**·10MeCN).

Given that mixed aluminum-lithium complexes have displayed favorable ROP characteristics *versus* their homo-metallic counterparts,<sup>[33]</sup> we treated the solution generated from  $\text{L}^8\text{H}_8$  and  $\text{LiOtBu}$  with  $\text{Me}_3\text{Al}$ . This led, following work-up, to the crystallization of the complex  $[(\text{AlMe}_2)_2\text{Li}_{20}(\text{L}^8\text{H}_2)_2(\text{OH}_2)_4(\text{O}^{2-})_4(\text{OH})_2(\text{NCMe})_{12}] \cdot 10\text{MeCN}$  (**5**·10MeCN). A representation of molecular structure is provided in Figure 8, along with selected bond lengths and angles in the caption. One quarter of the above formula comprises the asymmetric unit. The molecule resides on a center of symmetry and there is a mirror plane running long-ways through the molecule with all atoms having their  $y$ -coordinate = 0.0000 lying on the mirror, *i.e.* Li(4) > Li(7), O(1), O(5), & O(6), N(1), N(2), N(3), N(5), & N(7). The calix[8]arene is found to adopt a bowl conformation, whilst Li, O, Al, and N build a polyhedral center. Li(1), Li(2), Li(3), Li(5), Li(6),

Li(7), and Al(1) all make four bonds, however, Li(4) has five bonds (two views of the core are shown in Figure 9). H(7D) and H(7E) on the water link to N(4) on MeCN and O(8B), respectively via H-bonds. There is an intramolecular H-bond interaction between H(4) and O(3) within the calixarene. Li(4) makes a weak  $\pi$  interaction with the C(1) atom in the neighboring calixarene ring attached to O(1). The voids are filled with MeCN molecules between molecules of the complex. In the  $^1\text{H}$  NMR spectrum, the  $\text{AlMe}_2$  appears at  $\delta$  -0.81, whilst in the  $^7\text{Li}$  NMR spectrum, only 4 distinct lithium resonances are observed. In terms of charge, the 20+ available from the Li centers and the 2+ from the  $(\text{AlMe}_2)^+$  is balanced by 12- from the two calix[8]areneH<sub>2</sub>s and 8- from the four oxo anions and 2- from the two hydroxide anions.

### 3.2. Ring opening polymerization

*General:* With the track record of lithium-based systems for the ring opening polymerization (ROP) of cyclic esters in mind,<sup>[9,16,17]</sup> the ability of the complexes herein to perform as catalysts in the ROP of  $\epsilon$ -caprolactone ( $\epsilon$ -CL),  $\delta$ -valerolactone ( $\delta$ -VL), and *rac*-lactide (*r*-LA), in the presence of one equivalent of benzyl alcohol (BnOH) per lithium present, has been studied. Results are discussed versus reported calixarene complexes I – III (Chart 3).<sup>[9,34]</sup>

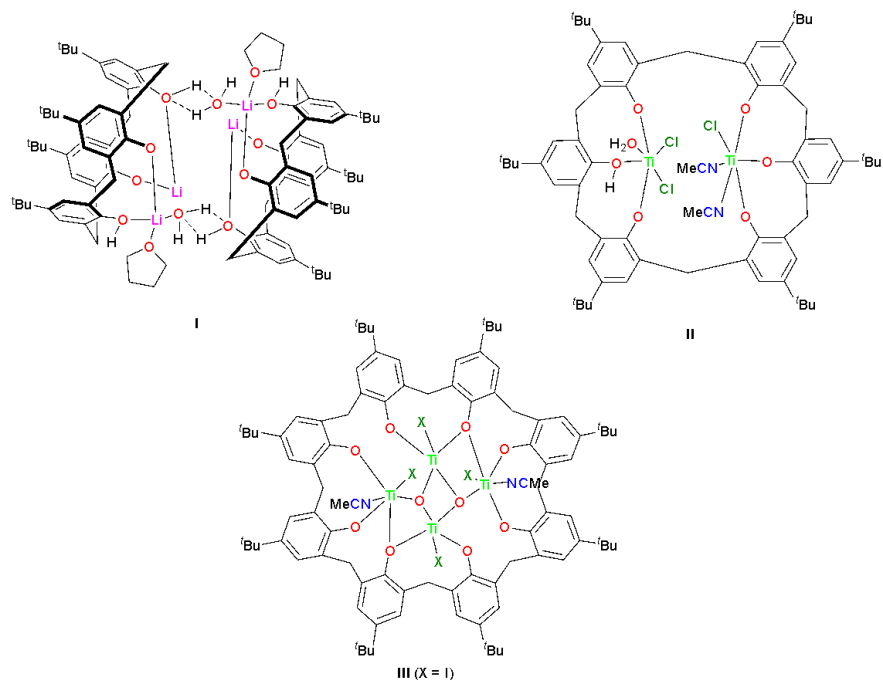


**Chart 3.** Literature complexes **I - III**. [9,34]

*ROP of  $\epsilon$ -caprolactone ( $\epsilon$ -CL)*

The complexes 1-5 were accessed for their potential to polymerize  $\epsilon$ -caprolactone and the results are collected in Table 1. The polymerization tests revealed that the optimum conditions comprised of 500 equivalents of  $\epsilon$ -caprolactone to lithium using a temperature of 130 °C. On increasing the temperature, the activity of **1** increased, whilst the use of 500 equivalents of monomer afforded the best conversions. Moreover, for **1** activity was also exhibited when using low catalyst loading achieving 56% conversion over 8 h when using 1000 equivalents of monomer. Highest conversion and molecular weight were achieved under no solvent conditions, with the run showing good control (Polydispersity Index PDI 1.18), which is consistent with former reports.<sup>[35]</sup> The polymers obtained possessed polydispersity < 1.85, whilst the  $M_n$  were far

lower than the respective calculated values, which suggested the occurrence of transesterification processes.<sup>[36]</sup>

The screening of **1-5** (Table 1; for  $M_n$ , cal, PDIs and TONs, see Table S1, ESI) revealed that under these conditions, the lithium/aluminum-based complex, namely **5**, could achieve higher activities when compared to the other complexes herein. From Table 4, it can be seen that complexes **1-4** afforded conversions <90% over 24h, whilst for **5**, higher conversions (>90%) were achieved under similar conditions. A kinetic study (Figure 6) revealed that the CL polymerization rate order is **5 > 1 > 2 > 3 > 4**. It is evident that the lithiated calix[6]arene complex **1** outperforms the complexes **2-4**, derived from calix[8]arenes; the latter were found to be relatively inactive (Table 1, entries 12-14). The observed activity of **5** was greater than that of the other complexes screened herein, which we attribute to the presence of the Al centres.<sup>[37-42]</sup> The enhanced activity of the **1** versus **2-4** we attribute to the lability of ligands present. This also reflects our observations when using titanocalix[4]arenes, where the labile ligand present (*i.e.* MeCN or H<sub>2</sub>O) appeared to benefit the catalyst activity.<sup>[43]</sup> <sup>1</sup>H NMR spectra of the polycaprolactone (PCL) revealed an BnO end group to be present (e.g. Figure S3, ESI). This is in agreement with the MALDI-ToF mass spectra (e.g. Figure S4, ESI) and is consistent with the polymerization proceeding via a coordination-insertion mechanism. The MALDI-ToF spectrum revealed a major family of peaks separated by 114 m/z units, consistent with two OH terminated PCL *n*-mers ( $M = 17 \text{ (OH)} + 1 \text{ (H)} + n \times 114.14 \text{ (CL)} + 45.98 \text{ (2Na}^+)$ ), whilst there is also a minor family of peaks assigned to the polymer terminated with OH and BnO end groups ( $M = n \times 114.12 \text{ (CL)} + 108.05 \text{ (BnOH)} + 45.98 \text{ (2Na}^+)$ ). Furthermore, the MALDI-ToF spectrum results also exhibited a

set of peaks assigned to cyclic PCL ( $M = n \times 114.12 \text{ (CL)} + 22.99 \text{ (Na}^+)$ ), which contributes about 25% of the afforded polymer product.

On comparison with the methylene-bridged lithiated calix[4]arene **I** (Chart 3, left), at 130 °C over 24h and using one equivalent of BnOH, a higher conversion for the systems herein is achieved (e.g. entries 4 and 21 *versus* entry 29, Table 1). In the absence of solvent, the conversion achieved by the mixed Al/Li system **5** over 1 h (entry 27) was somewhat less than that of **I** (entry 30) though with slightly better control. However, over 24h under air, the trend was reversed with **5** outperforming **I** (entries 25 v 31). In the case of the titanocalix[6 and 8]arenes **II** and **III**, complex **II** (entry 34) performs less well than those herein in terms of conversion affording in general lower molecular weight products but with slightly better control. The titanocalix[8]arene **III** performs slightly better than lithiated calix[8]arenes **3** and **4** (entries 35, 36) under the same conditions.

The active species in such lithiated systems is likely similar to that proposed for other multi-metallic lithium systems employing chelating phenoxides. For example, for the system derived from 2,2-ethylidene-bis(4,6-di-*tert*-butylphenol),<sup>[18]</sup> the ROP proceeds via monomer coordination to adjacent lithium centres and then attack by the benzyl alkoxy group (from addition of BnOH) at the ester carbonyl. A coordination-insertion mechanism thus proceeds. We have heated the clusters for longer periods (24h) at reflux in toluene- $d_8$ , and we see no changes in the  $^1\text{H}$  NMR spectra. We conclude from this that the clusters are thermally stable at the temperatures employed for the ROP runs.

**Table 1.** ROP of  $\epsilon$ -CL using **1 – 5** and **I-III**.

Entry	Cat	CL: Li: BnOH	t (h)	Conv <sup>a</sup> (%)	$M_{n,GPC} \times 10^{-3b}$	$M_w \times 10^{-3b}$	TOF (h <sup>-1</sup> ) <sup>c</sup>
1	<b>1</b>	1000: 1: 1	8	56.0	5.20	7.45	70
2	<b>1</b>	500: 1: 1	8	59.4	5.34	7.87	37
3	<b>1</b>	250: 1: 1	8	49.9	4.63	5.58	16
4	<b>1</b>	100: 1: 1	8	52.4	4.49	6.64	7
5 <sup>d</sup>	<b>1</b>	500: 1: 1	8	29.7	1.96	2.37	19
6 <sup>e</sup>	<b>1</b>	500: 1: 1	8	-	-	-	-
7	<b>2</b>	500: 1: 1	8	55.6	5.58	7.84	35
8	<b>3</b>	500: 1: 1	8	50.7	4.93	6.45	32
9	<b>4</b>	500: 1: 1	8	28.4	1.54	1.68	18
10	<b>5</b>	500: 1: 1	8	95.3	12.78	19.20	60
11	<b>1</b>	500: 1: 1	24	81.2	6.35	7.36	17
12	<b>2</b>	500: 1: 1	24	75.9	5.85	9.37	16
13	<b>3</b>	500: 1: 1	24	67.2	5.23	6.94	14
14	<b>4</b>	500: 1: 1	24	34.9	2.25	4.12	7
15	<b>5</b>	500: 1: 1	24	98.5	13.54	20.11	21
16	<b>1</b>	500: 1: 0	24	55.2	4.10	5.78	12
17	<b>2</b>	500: 1: 0	24	52.4	4.18	4.68	11
18	<b>3</b>	500: 1: 0	24	-	-	-	-
19	<b>4</b>	500: 1: 0	24	-	-	-	-
20	<b>5</b>	500: 1: 0	24	69.1	6.43	9.28	14
21	<b>5</b>	100: 1: 1	24	>99	9.85	12.95	4

22 <sup>f</sup>	<b>1</b>	100: 1: 0	24	74.5	7.61	8.41	3
23 <sup>f</sup>	<b>3</b>	100: 1: 0	24	60.7	6.82	7.69	3
24 <sup>f</sup>	<b>5</b>	100: 1: 0	24	>99	9.92	13.56	4
25 <sup>f,g</sup>	<b>5</b>	100: 1: 0	24	27.9	1.43	1.67	1
26 <sup>f</sup>	<b>5</b>	100: 1: 0	6	89.7	7.65	10.85	15
27 <sup>f</sup>	<b>5</b>	100: 1: 0	1	34.5	1.86	2.79	35
28 <sup>f</sup>	<b>5</b>	100: 1: 0	15 min.	15.4	0.72	0.95	62
29	<b>I</b>	100: 1: 1	24	20	-	-	0.8
30 <sup>f</sup>	<b>I</b>	100: 1: 0	1	80	16.13	28.71	80
31 <sup>f,g</sup>	<b>I</b>	100: 1: 0	24	14	-	-	0.6
32	<b>3</b>	500: 1: 3	24	75.4	5.24	7.21	16
33	<b>5</b>	500: 1: 3	24	>99	13.54	22.91	21
34	<b>II</b>	500: 1: 3	24	20	2.69	3.22	4
35	<b>3</b>	250: 1: 1	24	60.1	3.86	5.12	6
36	<b>4</b>	250: 1: 1	24	39.7	1.64	2.24	4
37	<b>III</b>	250: 1: 1	24	74	6.61	8.13	8

<sup>a</sup> Determined using <sup>1</sup>H NMR spectroscopy. <sup>b</sup> The values were corrected using the Mark–Houwink factor (0.56) from polystyrene standards in THF. <sup>c</sup> Turnover frequency (TOF) = TON/time (h). <sup>d</sup> Conducted at 100 °C. <sup>e</sup> Conducted at 80 °C. <sup>f</sup> Reaction performed without solvent. <sup>g</sup> Reaction performed in air.

### ROP of $\delta$ -valerolactone ( $\delta$ -VL)

Complexes **1-5** were also screened for their potential to act as catalysts, when using one equivalent of BnOH, in the ROP of  $\delta$ -VL (Table 2; for  $M_n$ ,cal, PDIs and TONs, see Table S1, ESI). Using **1**, the temperature and [Li]:[ $\delta$ -VL] ratio were varied. When elevating the temperature to 130 °C and on lowering the ratio of monomer to catalyst, best observed results were obtained at 130 °C for an [Li]:[ $\delta$ -VL] of 1:500 over 8 h. As observed for the ROP of  $\epsilon$ -CL, a kinetic study (Figure 11) yielded the catalytic activity order: **5 > 1 > 2 > 3 > 4**, and we assume the

same factors are at play here, *i.e.* labile ligation in **1** and the Al center in **5**. As in the case of the ROP of  $\epsilon$ -Cl, transesterification was evident and almost all observed  $M_n$  values were far lower than calculated values. MALDI-ToF mass spectra of the PVL (e.g. Figure S5, ESI) revealed a series (about 50%) of peaks consistent with a chain polymer bearing BnO and OH end groups [ $M = 108.05$  (BnOH) +  $n \times 100.12$  (VL) +  $22.99$  ( $\text{Na}^+$ )]. Furthermore, a second set of peaks (about 50%) were attributed to cyclic PVL [ $n \times 100.12$  (VL) +  $22.99$  ( $\text{Na}^+$ )]. The presence of a BnO end group was evident from the  $^1\text{H}$  NMR spectra of the PVL (e.g. Figure S6, ESI).

Comparison of **5** versus lithiated calix[4]arene **I** in the absence of solvent over 1 h (entries 13 v 18) indicated a better performance for **I**, with a slightly higher conversion, a larger molecular weight product and better control. In the case of the titanocalix[6]arene **II**, conversion is comparable with the lithiated complex **3** but inferior to the mixed-metal complex **5** (entries 19-21) under related conditions (only the amount of BnOH varied); **II** exhibited better control. For **III**, the trend was similar with better conversion shown by the mixed-metal system **5**, but poorer conversion seen for lithiated **3** under the same conditions.

**Table 2.** ROP of  $\delta$ -VL using **1** – **5** and **I-III**.

Entry	Cat.	VL: Li: BnOH	t (h)	Conv <sup>a</sup> (%)	$M_{n,\text{GPC}} \times 10^{-3b}$	$M_w \times 10^{-3b}$	TOF ( $\text{h}^{-1}$ )
1	<b>1</b>	1000: 1: 1	8	52.4	5.23	9.59	66
2	<b>1</b>	500: 1: 1	8	58.1	5.97	9.42	36
3	<b>1</b>	250: 1: 1	8	49.5	5.52	6.11	15
4	<b>1</b>	100: 1: 1	8	44.8	3.64	5.69	6
5 <sup>d</sup>	<b>1</b>	500: 1: 1	8	35.2	2.56	4.26	22
6 <sup>e</sup>	<b>1</b>	500: 1: 1	8	-	-	-	-
7	<b>2</b>	500: 1: 1	8	54.9	5.96	9.45	34

8	<b>3</b>	500: 1: 1	8	47.9	3.73	4.16	30
9	<b>4</b>	500: 1: 1	8	33.0	1.68	2.11	21
10	<b>5</b>	500: 1: 1	8	89.4	11.54	18.65	56
11 <sup>f</sup>	<b>5</b>	100: 1: 0	24	>99	15.69	16.56	4
12 <sup>f</sup>	<b>5</b>	100: 1: 0	12	96.1	12.14	14.33	8
13 <sup>f</sup>	<b>5</b>	100: 1: 0	1	36.5	2.12	4.45	37
14	<b>3</b>	500: 1: 3	24	62.1	4.85	6.24	13
15	<b>5</b>	500: 1: 3	24	>99	12.39	15.35	21
16	<b>3</b>	100: 1: 0	1	8.5	-	-	9
17	<b>5</b>	100: 1: 0	1	20.9	1.76	3.35	21
18 <sup>f</sup>	<b>I</b>	100: 1: 0	1	46.0	16.36	22.74	46
19	<b>II</b>	250: 1: 3	24	45.8	6.36	7.18	5
20	<b>3</b>	250: 1: 2	24	41.5	3.48	5.61	4
21	<b>5</b>	250: 1: 2	24	>99	8.93	15.19	10
22	<b>III</b>	250: 1: 2	24	69.6	13.00	17.81	7

<sup>a</sup> As determined using <sup>1</sup>H NMR spectroscopy. <sup>b</sup> The values were corrected using the Mark–Houwink factor (0.57) from polystyrene standards in THF. <sup>c</sup> Turnover frequency (TOF) = TON/time (h). <sup>d</sup> Conducted at 100 °C. <sup>e</sup> Conducted at 80 °C. <sup>f</sup> Reaction performed without solvent.

### *ROP of rac-lactide*

The lithiated species herein were also screened for their potential to act as catalysts for the ROP of *r*-LA (Table 3; for  $M_n$ , cal, PDIs and TONs, see Table S1, ESI). Best conversion was observed when using the aluminum complex **5** (56.6%, Table 3, entry 5), whilst for the lithiated calix[*n*]arenes **1** to **4**, the trend for conversions followed the order **1** > **2** > **3** > **4**. This is the same as the trend noted for both PCL and PVL formation, and again we put this down to either the presence of the more active aluminum centre (for **5**) or the presence of more labile ligands (in **1**) which allow for better access to the monomer. The observed polymer  $M_n$  value was smaller than

the calculated value albeit with narrow molecular weight distribution (6580 and 1.16, respectively). For systems **1-5**, all of the polymers obtained exhibited relatively narrow polydispersity ( $PDI < 1.75$ ), which we ascribe to moderate control of the polymerization process. However, use of complex **4** resulted in only 32.5% monomer conversion, and the isolation of low molecular weight species.  $^1\text{H}$  NMR spectra for the PLA samples revealed a BnO end group to be present (e.g. Figure S7, ESI), which is in agreement with the MALDI-ToF mass spectra (e.g. Figure S8, ESI). Analysis by MALDI-ToF mass spectra was conducted in the positive-linear mode with the expected series corresponding to repeating unit mass of 72/144 for half/full LA and a chain terminated by OH and BnO end groups [ $M = 108.05$  (BnOH) +  $n \times 72.06$  ( $\text{C}_3\text{H}_4\text{O}_2$ ) + 22.99 ( $\text{Na}^+$ )]. Furthermore, the MALDI-ToF spectrum also revealed a minor (*ca.* 10% of the total) peak series assigned to cyclic PCL ( $M = n \times 72.06$  ( $\text{C}_3\text{H}_4\text{O}_2$ ) + 22.99 ( $\text{Na}^+$ )). 2D *J*-resolved  $^1\text{H}$  NMR spectroscopy was employed to determine the syndiotactic bias; for the methine area (5.13-5.20 ppm) of the spectra, see for example Figure S9 (ESI).<sup>[44,45]</sup> The peaks/tetrads were assigned based on literature reports.<sup>[46,47]</sup> The observed value *Pr* (*Pr* = probability of racemic linkages) suggested all the catalysts afforded almost heteroatactic polymers.

Comparison *versus* lithiated **I** indicated that under solvent-free conditions (entries 7, 8) complex **5** outperforms **I**, whilst in toluene at 150°C, **5** exhibits comparable behavior to titanocalix[6]arene **II** (entries 9, 10) and outperforms **III** (entry 12) under the same conditions.

**Table 3.** ROP of *rac*-lactide over 24h using **1 – 5** and **I-III**.

Entry	Cat.	LA: Li: BnOH	T/°C	Conv <sup>a</sup> (%)	$M_{n,\text{GPC}} \times 10^{-3b}$	$M_w \times 10^{-3b}$	<i>Pr</i> <sup>c</sup>	TOF (h <sup>-1</sup> ) <sup>d</sup>
1	<b>1</b>	500: 1: 1	130	55.1	4.63	7.56	0.45	11

2	<b>2</b>	500: 1: 1	130	50.7	4.45	6.78	0.51	11
3	<b>3</b>	500: 1: 1	130	39.4	2.36	3.20	0.46	8
4	<b>4</b>	500: 1: 1	130	32.5	1.08	1.24	0.54	7
5	<b>5</b>	500: 1: 1	130	56.6	6.58	11.18	0.56	12
6	<b>5</b>	100: 1: 0	150	62.1	6.68	9.42	0.60	3
7	<b>5<sup>c</sup></b>	100: 1: 0	150	84.1	12.23	17.39	0.56	4
8	<b>I<sup>c</sup></b>	100: 1: 0	150	18	-	-	-	1
9	<b>5</b>	500: 1: 3	150	85.6	8.23	12.52	0.45	18
10	<b>II</b>	500: 1: 3	150	87	8.19	10.56	0.51	18
11	<b>5</b>	250: 1: 1	150	91.4	7.55	10.52	0.45	10
12	<b>III</b>	250: 1: 1	150	8.2	-	-	-	1

<sup>a</sup> As determined using <sup>1</sup>H NMR spectroscopy of the crude reaction mixture. <sup>b</sup> The values were corrected using the Mark–Houwink factor (0.58) from polystyrene standards in THF. <sup>c</sup> Using 2D *J*-resolved <sup>1</sup>H NMR spectroscopy. <sup>d</sup> Turnover frequency (TOF) = TON/time (h). <sup>e</sup> Solvent free conditions.

### *ROP of $\omega$ -pentadecalactone*

In order to improve the polymers thermal properties, the ROP of the  $\omega$ -pentadecalactone was also investigated. However, the systems herein proved to be ineffective as catalysts for the ROP of  $\omega$ -pentadecalactone either as melts or at elevated temperatures (130 °C) in solution.

### *Kinetics*

A kinetic study on the ROP of  $\epsilon$ -CL for 1-5 revealed that the polymerization rate exhibited first-order dependence on  $\epsilon$ -CL concentration (Figure 10(a)), and the monomer conversion observed over 420 min was >20%. In this case, the activity trend revealed that 5 exhibited the highest activity with the order as 5 > 1 > 2 > 3 > 4. For all complexes, an induction period of 2 h is

observed, and this is ascribed to the time needed to form the catalytically active species; a similar situation was evident for  $\delta$ -VL polymerization (Figure 11).

The  $M_n$  and molecular weight distribution dependence on the monomer conversion in the reactions catalyzed by 1, 3, 5 with BnOH was probed (Figure 12). For  $\epsilon$ -CL, the  $M_n$  of the polymer was found to increase in linear fashion with conversion, and this is consistent with a well-controlled polymerization (Figure 12, left); the situation observed using  $\delta$ -VL was similar (Figure 12, right).

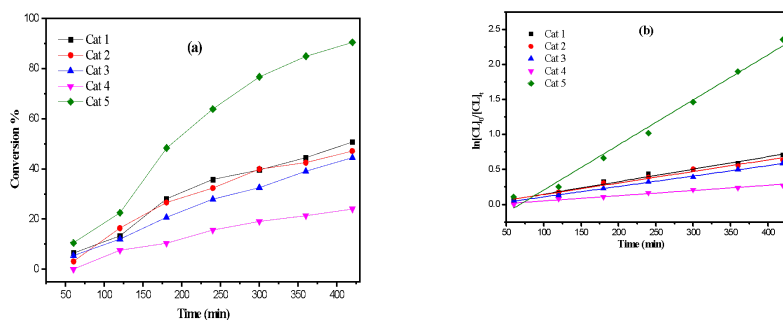


**Figure 10.** (a) The relationship between conversion and time in the ROP of  $\epsilon$ -CL using complexes 1-5; (b) Plot of  $\ln[CL]_0/[CL]_t$  vs. time for the ROP of  $\epsilon$ -CL using 1-5; Conditions:  $T=130\text{ }^\circ\text{C}$ ,  $n_{\text{Monomer}}:n_{\text{Li}}:\text{BnOH}=500:1:1$ .

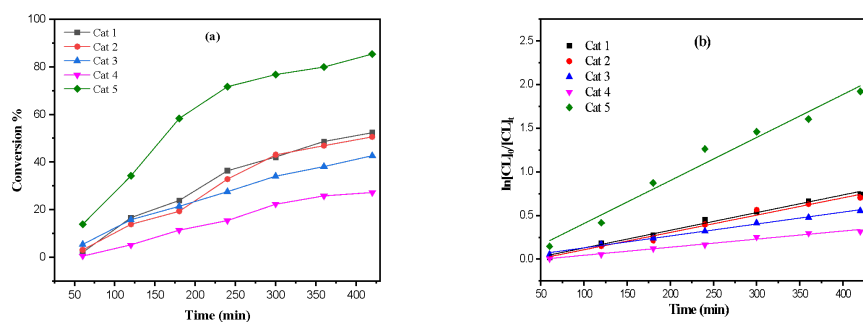


**Figure 11.** (a) The relationship between conversion and time for the ROP of  $\delta$ -VL using complexes 1-5; (b) Plot of  $\ln[VL]_0/[VL]_t$  vs. time for the ROP of  $\delta$ -VL using 1-5; Conditions:  $T=130\text{ }^\circ\text{C}$ ,  $n_{\text{Monomer}}:n_{\text{Li}}:\text{BnOH}=500:1:1$ .

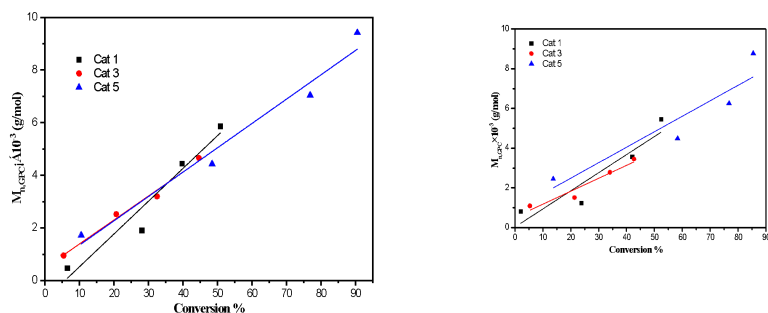


**Figure 12.** Left: A plot of  $M_n$  vs. monomer conversion for the ROP of  $\epsilon$ -CL using 1, 3 and 5; Right: A plot of  $M_n$  vs. monomer conversion in the ROP of  $\delta$ -VL using 1, 3 and 5; Conditions:  $T=130\text{ }^\circ\text{C}$ ,  $n_{\text{Monomer}}:n_{\text{Li}}:\text{BnOH}=500:1:1$

#### 4. Conclusion

In this work, rare examples of lithium complexes of larger *p-tert*-butylcalix[*n*]arenes ( $n = 6, 8$ ) are reported. The molecular structures reveal how flexible these macrocycles can be, and emphasize their ability to simultaneously support multiple metal centers, which leads to the

adoption of some interesting structural motifs. The complexes proved active in the ROP of  $\epsilon$ -caprolactone ( $\epsilon$ -CL),  $\delta$ -valerolactone ( $\delta$ -VL) and *rac*-lactide (*r*-LA), with the mixed lithium-aluminum complex  $[(\text{AlMe}_2)_2\text{Li}_{20}(\text{L}^8\text{H}_2)_2(\text{OH}_2)_4(\text{O}^{2-})_4(\text{OH})_2(\text{NCMe})_{12}]\cdot 10\text{MeCN}$  (**5**·10MeCN) proving to be the most active and exhibiting first order kinetics. Low molecular weight products were obtained but with good control.

#### ASSOCIATED CONTENT

**Supporting information:** The supporting information including: (1) Alternative views of the cores of the structures **2**·7THF and **4**·5.5THF; (2) Crystallographic parameters for Li complexes **1** - **5**. (3) Additional ROP data including  $M_n$  calc, PDI and TON for PCL, PVL and PLA screening; (4)  $^1\text{H}$  NMR and 2D *J*-resolved  $^1\text{H}$  NMR spectrum for afforded PCL, PVL and PLA; (5) Mass spectrum for the afforded PCL, PVL and PLA.

**Accession codes:** CCDC 2084708-2084712 contain the supplementary crystallographic data for 1-3. These data can be obtained free of charge via <http://www.ccdc.cam.ac.uk/conts/retrieving.html> or from the Cambridge Crystallographic Data Centre, 12 Union Road, Cambridge, CB2 1EZ, UK; fax (+44) 1223-336-033; or e-mail: [deposit@ccdc.cam.ac.uk](mailto:deposit@ccdc.cam.ac.uk).

#### Author Contributions

Tian Xing: Investigation; Writing; Chengying Jiang: Investigation; Mark R. J. Elsegood: Investigation for crystal structure; Carl Redshaw: Supervision; Writing, Editing and Funding acquisition.

## **Acknowledgements**

We thank the China Scholarship Council (CSC) for a PhD Scholarship to TX. CR thanks the EPSRC for funding (EPS025537/1), and the EPSRC National Crystallography Service at Southampton (UK) and the Mass Spectrometry Service Centre, Swansea (UK) for data.

## AUTHOR INFORMATION

### **Corresponding Author**

Carl Redshaw – Plastics Collaboratory, Department of Chemistry, University of Hull, Hull, HU6 7RX, U.K. [orcid.org/0000-0002-2090-1688](https://orcid.org/0000-0002-2090-1688) Email. [C.Redshaw@hull.ac.uk](mailto:C.Redshaw@hull.ac.uk)

### **Authors**

Tian Xing – Plastics Collaboratory, Department of Chemistry, University of Hull, Hull, HU6 7RX, U.K.

Chengying Jiang, – Chemistry Department, Loughborough University, Loughborough, Leicestershire, LE11 3TU, U.K.

Mark R. J. Elsegood – Chemistry Department, Loughborough University, Loughborough, Leicestershire, LE11 3TU, U.K.

## Funding Sources

PhD funding from China Scholarship Council (CSC).

UKRI Creative Circular Plastic Grant (EPS025537/1).

## Notes

The authors declare no potential conflict of interest.

## REFERENCES

[1] Jose P.; Menon S. Lower-rim substituted calixarenes and their applications, *Bioinorg. Chem. Appl.* **2007**, 2007, 1-16.

[2] Nimse S. B.; Kim T. Biological applications of functionalized calixarenes, *Chem. Soc. Rev.* **2013**, 42, 366-386.

[3] Li Y.; Zhao K.-Q.; Redshaw C.; Martínez Ortega B. A.; Nuñez A. Y.; Hanna T. A. 'Coordination Chemistry and Applications of Phenolic Calixarene–metal Complexes'. Patai's Chemistry of Functional Groups. Wiley **2014**; pp 1-164.

[4] Deska M.; Dondela B.; Silwa W. Selected applications of calixarene derivatives, *Arkivov* **2015**, vi, 393-416.

- [5] Kumar R.; Sharma A.; Singh H.; Suating P.; Kim H. S.; Sunwoo K.; Shim I.; Gibb B. C.; Kim J. S. Revisiting fluorescent calixarenes: from molecular sensors to smart materials, *Chem. Rev.* **2019**, 119, 9657-9721.
- [6] Wang J.; Zhuang S. Cesium separation from radioactive waste by extraction and adsorption based on crown ethers and calixarenes, *Nucl. Eng. Technol.* **2020**, 52, 328-336.
- [7] Ikeda A.; Shinkai S. Novel cavity design using calix[n]arene skeletons: toward molecular recognition and metal Binding, *Chem. Rev.* **1997**, 97, 1713-1734.
- [8] Homden D. M.; Redshaw C. The use of calixarenes in metal-based catalysis, *Chem. Rev.* **2008**, 108, 5086-5130.
- [9] Santoro O.; Elsegood M. R. J.; Teat S. J.; Yamato T.; Redshaw C. Lithium calix[4]arenes: structural studies and use in the ring opening polymerization of cyclic esters, *RSC Adv.* **2021**, 11, 11304-11317.
- [10] Raquez J. -M.; Mincheva R.; Coulembier O.; Dubois P. Ring-opening Polymerization of Cyclic Esters: Industrial Synthesis, Properties, Applications, and Perspectives. In *Polymer Science: A Comprehensive Reference*; Elsevier: Amsterdam, The Netherlands, **2012**; pp. 761-777.
- [11] Redshaw C.; Coordination chemistry of the larger calixarenes, *Coord. Chem. Rev.* **2003**, 244, 45-70.

- [12] Wang K.; Prior T. J.; Redshaw C. Turning on ROP activity in a bimetallic Co/Zn complex supported by a [2+ 2] Schiff-base macrocycle, *Chem. Commun.* **2019**, 55, 11279-11282.
- [13] Clague N. P.; Crane J. D.; Moreton D. J.; Sinn E.; Teat S. J.; Young N. A. A mixed lithium–strontium polynuclear complex formed within the hexa-deprotonated calix[8]arene framework; the synthesis and structure of  $\text{Li}_4\text{Sr}_2(\text{H}_2\text{L})(\text{O}_2\text{CC}_4\text{H}_9)_2(\text{dmf})_8$  [ $\text{H}_8\text{L} = p\text{-Pr}^i\text{-}$  or  $p\text{-Bu}^i\text{-calix[8]arene}$ ], *J. Chem. Soc., Dalton Trans.*, 1999, 3535-3536.
- [14] Bergougnant R. D.; Robin A. Y.; Fromm K. M. From simple rings to one-dimensional channels with calix[8]arenes, water clusters, and alkali metal ions, *Tetrahedron* **2007**, 63, 10751-10757.
- [15] For example, as of 17.6.21 on the Sigma-Aldrich website, the cost of  $\text{L}^8\text{H}_8 = 5 \text{ g}$  for £46.60 (USD 64.94);  $\text{L}^6\text{H}_6 = 5 \text{ g}$  for £130 (USD 181.17);  $\text{deBuL}^8\text{H}_8 = 1 \text{ g}$  for £57.50 (USD 80.14).
- [16] Sutar A. K.; Maharana T.; Dutta S.; Chen C. -T. Ring-opening polymerization by lithium catalysts: an overview, *Chem. Soc. Rev.* **2010**, 39, 1724-1746.
- [17] Gao J.; Zhu D.; Zhang W.; Solan G. A.; Ma Y.; Sun W. -H. Recent progress in the application of group 1, 2 & 13 metal complexes as catalysts for the ring opening polymerization of cyclic esters, *Inorg. Chem. Front.* **2019**, 6, 2619-2652.
- [18] Ko B. -T.; Lin C. -C. Synthesis, characterization, and catalysis of mixed-ligand lithium aggregates, excellent initiators for the ring-opening polymerization of *l*-Lactide, *J. Am. Chem. Soc.* **2001**, 123, 7973-7977.

[19] Chisholm M. H.; Lin C. –C.; Gallucci J. C.; Ko B. –T. Binolate complexes of lithium, zinc, aluminium, and titanium; preparations, structures, and studies of lactide polymerization, *Dalton Trans.* **2003**, 406-412.

[20] Huang C. –A.; Chen C. –T. Lithium complexes supported by amine bis-phenolate ligands as efficient catalysts for ring-opening polymerization of *l*-lactide, *Dalton Trans.* **2007**, 5561-5566.

[21] Clegg W.; Davidson M. G.; Graham D. V.; Griffen G.; Jones M. D.; Kennedy A. R.; O'Hara C. T.; Russo L.; Thomson C. M. Synthetic and structural investigations of alkali metal diamine bis(phenolate) complexes, *Dalton Trans.* **2008**, 1295-1301.

[22] Huang Y.; Tsai Y. –H.; Hung W. –C.; Lin C. –S.; W. Wang; Huang J. –H.; Dutta S.; Lin C. –C. Synthesis and structural studies of lithium and sodium complexes with OOO-tridentate bis(phenolate) ligands: effective catalysts for the ring-opening polymerization of *l*-lactide, *Inorg. Chem.* **2010**, 49, 9416-9425.

[23] Lu W. –Y.; Hsiao M. –W.; Hsu S. C. N.; Peng W. –T.; Chang Y. –J.; Tsou Y. –C.; Wu T. –Y.; Lai Y. –C.; Chen Y.; Chen H. –Y. Synthesis, characterization and catalytic activity of lithium and sodium iminophenoxide complexes towards ring-opening polymerization of *l*-lactide, *Dalton Trans.* **2012**, 41, 3659-3667.

[24] Ikpo N.; Hoffmann C.; Dawe L. N.; Kerton F. M.; Ring-opening polymerization of  $\epsilon$ -caprolactone by lithium piperazinyl-aminephenolate complexes: synthesis, characterization and kinetic studies, *Dalton Trans.* **2012**, 41, 6651-6660.

- [25] Dean R. K.; Reckling A. M.; Chen H.; Dawe L. N.; Schneider C. M.; Kozak C. M. Ring-opening polymerization of cyclic esters with lithium amine-bis(phenolate) complexes, *Dalton Trans.* **2013**, 42, 3504-3520.
- [26] Alhashmialameer D.; Ikpo N.; Collins J.; Dawe L. N.; Hattenhauer K.; Kerton F. M. Ring-opening polymerization of rac-lactide mediated by tetrametallic lithium and sodium diamino-bis (phenolate) complexes, *Dalton Trans.* **2015**, 44, 20216-20231.
- [27] Devaine-Pressing K.; Oldenburg F. J.; Menzel J. P.; Springer M.; Dawe L. N.; Kozak C. M. Lithium, sodium, potassium and calcium amine-bis (phenolate) complexes in the ring-opening polymerization of *rac*-lactide, *Dalton Trans.* **2020**, 49, 1531-1544.
- [28] Sheldrick G. M. SHELXT - Integrated space-group and crystal-structure determination, *Acta Cryst.* **2015**, A71, 3-8.
- [29] Spek A. L.; PLATON SQUEEZE: a tool for the calculation of the disordered solvent contribution to the calculated structure factors, *Acta Cryst.* **2015**, C71, 9-18.
- [30] Sluis P. v. d.; Spek A. L. BYPASS: an effective method for the refinement of crystal structures containing disordered solvent regions, *Acta Cryst.* **1990**, A46, 194-201.
- [31] Gueneau E. D.; Fromm K. M.; Goesmann H. Synthesis and structural analysis of the polymetallated alkali calixarenes  $[M_4(p\text{-tert-butylcalix}[4]\text{arene-4H})(\text{thf})_x]_2 \cdot n \text{ THF}$  (M=Li, K;  $n=6$  or 1;  $x=4$  or 5) and  $[\text{Li}_2(p\text{-tert-butylcalix}[4]\text{arene-2H})(\text{H}_2\text{O})(\mu\text{-H}_2\text{O})(\text{thf})] \cdot 3 \text{ THF}$ , *Chem. Eur. J.* **2003**, 9, 509-514.

- [32] McLellan R.; Rezé J.; Taylor S. M.; McIntosh R. D.; Brechin E. K.; Dalgarno S. J. Discovering the pivotal role of carbonate in the formation of a bis-phenolate supported Co<sub>15</sub> cluster, *Chem. Commun.* **2014**, 50, 2202-2204.
- [33] Muñoz M. T.; Cuenca T.; Mosquera M. E. G. Heterometallic aluminates: alkali metals trapped by an aluminum aryloxide claw, *Dalton Trans.* **2014**, 43, 14377-14385.
- [34] Santoro O.; Elsegood M. R. J.; Bedwell E. V.; Pryce J. A.; Redshaw C. INSIGHTS into the structures adopted by titanocalix[6 and 8]arenes and their use in the ring opening polymerization of cyclic esters, *Dalton Trans.* **2020**, 49, 11978-11996.
- [35] Chmura A. J.; Davidson M. G.; Frankis C. J.; Jones M. D.; Lunn M. D. Highly active and stereoselective zirconium and hafnium alkoxide initiators for solvent-free ring-opening polymerization of *rac*-lactide, *Chem. Commun.*, **2008**, 1293-1295.
- [36] Frediani M.; Sémeril D.; Marriotti A.; Rosi L.; Frediani P.; Rosi L.; Matt D.; Toupet L. Ring opening polymerization of lactide under solvent -free conditions catalyzed by a chlorotitanium calix[4]arene complex, *Macromol. Rapid Comm.*, **2008**, 29, 1554-1560.
- [37] Wei Y.; Wang S.; Zhou S. Aluminum alkyl complexes: synthesis, structure, and application in ROP of cyclic esters, *Dalton Trans.* **2016**, 45, 4471–4485.
- [38] Fuoco T.; Pappalardo D. Aluminum alkyl complexes bearing salicylaldiminato ligands: versatile initiators in the ring-opening polymerization of cyclic esters, *Catalysts* **2017**, 7, 64–81.

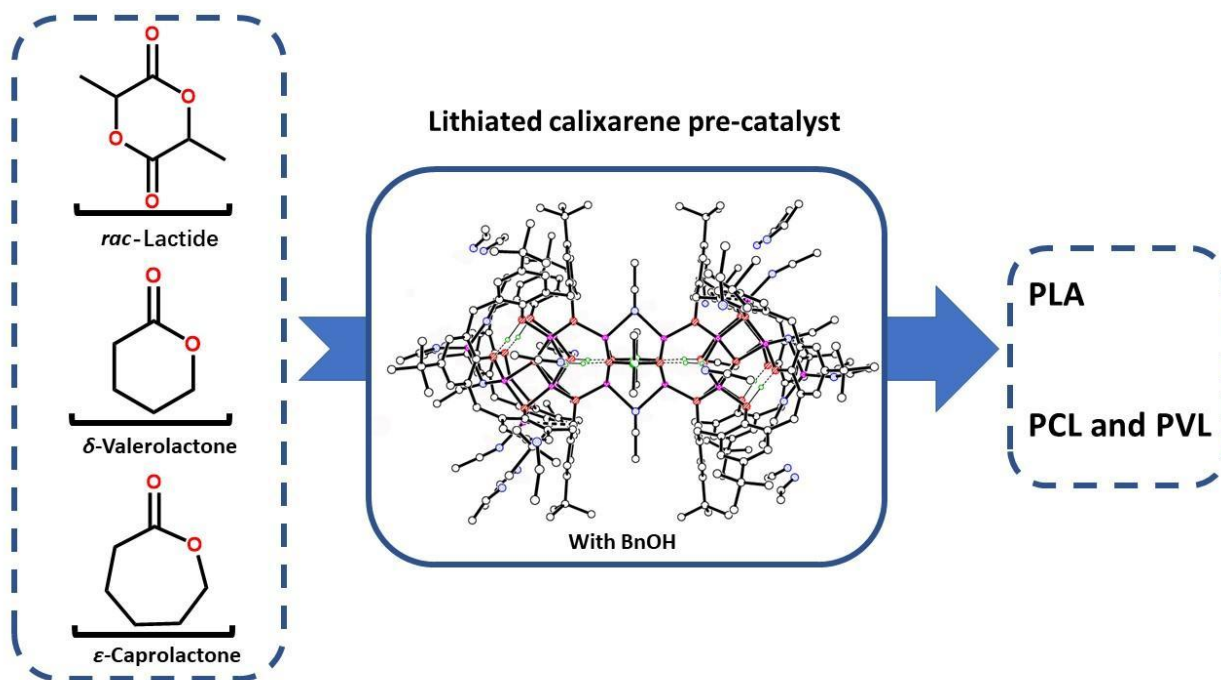
- [39] Li Y.; Zhao K.-Q.; Elsegood M. R. J.; Prior T. J.; Sun X.; Mo S.; Redshaw C. Organoaluminium complexes of *ortho*-, *meta*-, *para*-anisidines: synthesis, structural studies and ROP of  $\epsilon$ -caprolactone (and *rac*-lactide), *Catal. Sci. Technol.* **2014**, 4, 3025–3031
- [40] Antelmann B.; Chisholm M. H.; Iyer S. S.; Huffman J. C.; Navarro-Llobet D.; Pagel M.; W. Simonsick J.; Zhong W. Molecular Design of Single Site Catalyst Precursors for the Ring-Opening Polymerization of Cyclic Ethers and Esters. 2.<sup>1</sup> Can Ring-Opening Polymerization of Propylene Oxide Occur by a Cis-Migratory Mechanism?, *Macromolecules*, **2001**, 34, 3159–3175.
- [41] Braune W.; Okuda J. An efficient method for controlled propylene oxide polymerization: the significance of bimetallic activation in aluminum Lewis acids, *Angew. Chem. Int. Ed.* **2003**, 42, 64–68.
- [42] Redshaw C. Use of metal catalysts bearing Schiff base macrocycles for the ring opening polymerization (ROP) of cyclic esters, *Catalysts* **2017**, 7, 165-175.
- [43] Sun Z.; Zhao Y.; Santoro O.; Elsegood M. R. J.; Bedwell E. V.; Zahra K.; Walton A., Redshaw C. Use of titanocalix[4]arenes in the ring opening polymerization of cyclic esters, *Catal. Sci. Technol.* **2020**, 10, 1619-1639.
- [44] Ludwig C.; Viant M. R. Two-dimensional J-resolved NMR spectroscopy: review of a key methodology in the metabolomics toolbox, *Phytochem. Anal.* **2010**, 21, 22-32.

[45] Walton M. J.; Lancaster S. J.; Redshaw C. Highly selective and immortal magnesium calixarene complexes for the ring-opening polymerization of *rac*-lactide, *ChemCatChem* **2014**, 6, 1892-1898.

[46] Zhong Z.; Dijkstra P. J.; Feijen J. Controlled and stereoselective polymerization of lactide: kinetics, selectivity, and microstructures, *J. Am. Chem. Soc.* **2003**, 125, 11291-11298.

[47] Hormnirun P.; Marshall E. L.; Gibson V. C.; A. White J. P.; Williams D. J. Remarkable stereocontrol in the polymerization of racemic lactide using aluminum initiators supported by tetradentate aminophenoxide ligands, *J. Am. Chem. Soc.* **2004**, 126, 2688-2689.

## Table of Content



Calix[*n*]arenes (*n* = 6 or 8) ligand have been complexed with Li, and used as catalyst for ring opening polymerization of cyclic esters.